SOME PROBLEMS IN THE THEORY OF NONLINEAR OSCILLATIONS

YOSHISUKE UEDA

1968

Some Problems in the Theory of Nonlinear Oscillations

SOME PROBLEMS IN THE THEORY OF NONLINEAR OSCILLATIONS

YOSHISUKE UEDA, D. ENG.
DEPARTMENT OF ELECTRICAL ENGINEERING
KYOTO UNIVERSITY, KYOTO, JAPAN

NIPPON PRINTING AND PUBLISHING COMPANY, LTD.
OSAKA, JAPAN
1968

This monograph is a part of the author's doctrial thesis submitted to the Faculty of Engineering, Kyoto University, in February, 1965. The thesis was supervised by Professor C. Hayashi. The members of the thesis committee were Professors C. Hayashi, S. Hayashi, and B. Kondo.

NIPPON PRINTING AND PUBLISHING COMPANY, LTD.
KIKKO-CHO 2, FUKUSHIMA-KU, OSAKA, JAPAN

PRINTED IN JAPAN

PREFACE

This book is devoted to the study of nonlinear oscillations in certain types of physical systems and consists of three chapters. The first two chapters describe the generation of higher-harmonic oscillations which predominantly occur in some electrical systems. Chapter 1 is concerned with a series-resonance circuit containing a saturable inductor and a capacitor in series. The differential equation which describes the system takes the form of Duffing's equation. Chapter 2 treats higher-harmonic oscillations in an electrical system in which two parallel-resonance circuits are connected in series. The differential equation of the system is given by Mathieu's equation with an additional nonlinear term. The final chapter is devoted to the investigation of almost periodic oscillations which occur in a self-oscillatory system under periodic excitation. The system governed by van der Pol's equation with forcing term is treated. In all chapters, the relationship between the regions of the system parameters and the resulting responses of different types is investigated by applying the well-known methods of analysis. The stability of these responses is also discussed by considering variational equations. Furthermore, numerical analyses of the system equations for some representative values of parameters are carried out by using computer of either the analog or the digital type.

This monograph is a part of the author's dissertation on nonlinear oscillations submitted to the Faculty of Engineering in 1965 under the guidance of Dr. C. Hayashi, Professor of Kyoto University. The author wishes to express sincere gratitude for his constant and generous guidance and encouragement for many years during which the work was in progress. The author's thanks are also due to Dr. Y. Nishikawa and Dr. M. Abe, both Assistant Professors of Kyoto University, for their valuable advices and good guidances.

In the preparation of the present book the author was greatly aided by Assistant Professor Dr. T. Ozawa, and by Mr. H. Kawakami, who gave him valuable suggestions and many good advices of all kinds.

The publication of this book was greatly facilitated by the Grant in Aid of the Ministry of Education of Japan for Publishing Research Result and by the generous support of the Nippon Printing and Publishing Company. The KDC-I Digital Computer Laboratory of Kyoto University has made computer-time available to the author. The author wishes to acknowledge the kind considerations of the staffs of these organizations. Finally, the author wishes to thank the Sakkokai Foundation for a fund of research-aid in promoting this investigation.

January, 1968 YOSHISUKE UEDA

CONTENTS

CHAPTER 1

HIGHER-HARMONIC OSCILLATIONS IN A SERIES-RESONANCE CIRCUIT

1.1 Introduction

Under the action of a sinusoidal external force, a nonlinear system may exhibit basically different phenomena from those found in linear systems. One of the salient features of such phenomena is the generation of higher harmonics and subharmonics. A considerable number of papers have been published concerning subharmonic oscillations in nonlinear systems [13, 23]; however, very few investigations have been reported on the generation of higher harmonics.

This chapter deals with higher harmonic oscillations which predominantly occur in a series-resonance circuit containing a saturable inductor and a capacitor in series. The differential equation which describes the system takes the form of Duffing's equation. The solutions of this equation are studied both by using harmonic balance method and by using mapping procedure.

An experimental result using a series-resonance circuit is to be found in the work of Prof. C. Hayashi [13]. His result is cited at the end of this chapter.

1.2 Derivation of the Fundamental Equation

The schematic diagram illustrated in Fig. 1.1 shows an electrical circuit in which the nonlinear oscillation takes place due to the saturable-core inductance L under the impression of the alternating voltage $E \sin \omega t$. As shown in the figure, the resistor R is paralleled with the capacitor C, so that the circuit is dissipative. With the notation of the figure, the equations for the circuit are written as

$$\begin{aligned} n\frac{d\phi}{dt}+Ri_R &= E \sin \omega t \\ Ri_R = \frac{1}{C}\int i_C dt \qquad & i = i_R + i_C \end{aligned} \tag{1.1}$$

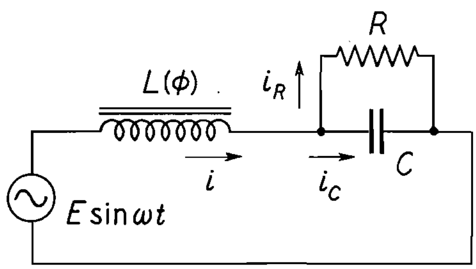

FIG. 1.1 Series-resonance circuit with nonlinear inductance.

where n is the number of turns of the inductor coil, and ϕ is the magnetic flux in the core. Then, neglecting hysteresis, we may assume the saturation curve of the form

$$i = a_1\phi + a_3\phi^3 \tag{1.2}$$

where higher powers of ϕ than the third are neglected. We introduce dimensionless variables u and v, defined by

$$i = I\cdot u \qquad \phi = \Phi\cdot v \tag{1.3}$$

where I and Φ are appropriate base quantities of the current and the flux, respectively. Then Eq. (1.2) becomes

$$u = \frac{a_1\Phi}{I}v + \frac{a_3\Phi^3}{I}v^3 = c_1 v + c_3 v^3 \tag{1.4}$$

Although the base quantities I and Φ can be chosen quite arbitrarily, it is preferable, for the brevity of expression, to fix them by the relations

$$n\omega^2 C\Phi = I \qquad c_1 + c_3 = 1 \tag{1.5}$$

Then, after elimination of i_R and i_C in Eqs. (1.1) and use of Eqs. (1.3), (1.4), and (1.5), the result in terms of v is

$$\frac{d^2v}{d\tau^2} + k\frac{dv}{d\tau} + c_1 v + c_3 v^3 = B\cos\tau \tag{1.6}$$

where $\qquad \tau = \omega t - \tan^{-1}k \qquad k = \dfrac{1}{\omega CR} \qquad B = \dfrac{E}{n\omega\Phi}\sqrt{1+k^2}$

Equation (1.6) is a well-known equation in the theory of nonlinear oscillations and is known as Duffing's equation [11].

1.3 Solution of the Fundamental Equation Using Principle of Harmonic Balance

(a) Periodic Solution Consisting of Odd-order Harmonics

As the amplitude B of the external force increases, an oscillation develops in which higher harmonics may not be ignored in comparison with the fundamental component. Since the system is symmetrical, we assume, for the time being, that these higher harmonics are of odd orders; hence a periodic solution for Eq. (1.6) may be written as

$$v_0(\tau) = x_1\sin\tau + y_1\cos\tau + x_3\sin 3\tau + y_3\cos 3\tau \tag{1.7}$$

Terms of harmonics higher than the third are certain to be present but are ignored to this order of approximation.

The coefficients in the right side of Eq. (1.7) may be found by the method of harmonic balance [9, 13]; that is, substituting Eq. (1.7) into (1.6) and equating the coefficients of the terms containing sin τ, cos τ, sin 3τ, and cos 3τ separately to zero yields

$$\begin{aligned} -A_1x_1-ky_1-\tfrac{3}{4}c_3[(x_1^2-y_1^2)x_3+2x_1y_1y_3] &\equiv X_1(x_1, y_1, x_3, y_3) = 0 \\ kx_1-A_1y_1+\tfrac{3}{4}c_3[2x_1y_1x_3-(x_1^2-y_1^2)y_3] &\equiv Y_1(x_1, y_1, x_3, y_3) = B \\ -A_3x_3-3ky_3-\tfrac{1}{4}c_3(x_1^2-3y_1^2)x_1 &\equiv X_3(x_1, y_1, x_3, y_3) = 0 \\ 3kx_3-A_3y_3-\tfrac{1}{4}c_3(3x_1^2-y_1^2)y_1 &\equiv Y_3(x_1, y_1, x_3, y_3) = 0 \end{aligned} \tag{1.8}$$

where $A_1 = 1-c_1-\tfrac{3}{4}c_3(r_1^2+2r_3^2) \quad A_3 = 9-c_1-\tfrac{3}{4}c_3(2r_1^2+r_3^2)$

$r_1^2 = x_1^2+y_1^2 \qquad r_3^2 = x_3^2+y_3^2$

Elimination of the x and y components in the above equations gives

$$\begin{aligned} \left[\left(A_1-\frac{3r_3^2}{r_1^2}A_3\right)^2+k^2\left(1+\frac{9r_3^2}{r_1^2}\right)^2\right]r_1^2 &= B^2 \\ (A_3^2+9k^2)r_3^2 &= \tfrac{1}{16}c_3^2r_1^6 \end{aligned} \tag{1.9}$$

From these relations the components r_1 and r_3 of the periodic solution are determined. By use of Eqs. (1.8) and (1.9) the coefficients of the periodic solution are found to be

$$x_1 = \frac{k(r_1^2+9r_3^2)}{B} \qquad y_1 = \frac{-(A_1r_1^2-3A_3r_3^2)}{B} \tag{1.10}$$

and

$$x_3 = \frac{4r_3^2}{c_3r_1^6}[-PA_3+3kQ] \qquad y_3 = \frac{4r_3^2}{c_3r_1^6}[-QA_3-3kP] \tag{1.11}$$

where $P = (x_1^2-3y_1^2)x_1 \qquad Q = (3x_1^2-y_1^2)y_1$

(*b*) *Stability Investigation of the Periodic Solution*

The periodic states of equilibrium determined by Eqs. (1.7), (1.10), and (1.11) are not always realized, but are sustained actually if they are stable. In this section the stability of the periodic solution will be investigated by considering the behavior of a small variation $\xi(\tau)$ from the periodic solution $v_0(\tau)$. If this variation $\xi(\tau)$ tends to zero with increasing τ, the periodic solution is stable (asymptotically stable in the sense of Lyapunov [27]); if $\xi(\tau)$ diverges, the periodic solution is unstable. Let $\xi(\tau)$ be a small variation defined by

$$v(\tau) = v_0(\tau)+\xi(\tau) \tag{1.12}$$

Substituting Eq. (1.12) into (1.6) and neglecting terms of higher degree than the first in ξ, we obtain the variational equation

$$\frac{d^2\xi}{d\tau^2}+k\frac{d\xi}{d\tau}+(c_1+3c_3v_0^2)\xi = 0 \tag{1.13}$$

Introducing a new variable $\eta(\tau)$ defined by

$$\xi(\tau) = e^{-\delta\tau}\cdot\eta(\tau) \qquad \delta = k/2 \tag{1.14}$$

yields

$$\frac{d^2\eta}{d\tau^2}+(c_1-\delta^2+3c_3v_0^2)\eta = 0 \tag{1.15}$$

in which the first-derivative term has been removed. Inserting $v_0(\tau)$ as given by Eq. (1.7) into (1.15) leads to a Hill's equation of the form

$$\frac{d^2\eta}{d\tau^2}+\left(\theta_0+2\sum_{n=1}^{3}\theta_{ns}\sin 2n\tau+2\sum_{n=1}^{3}\theta_{nc}\cos 2n\tau\right)\eta = 0 \tag{1.16}$$

where

$$\begin{aligned}
&\theta_0 = c_1-\delta^2+\tfrac{3}{2}c_3(r_1^2+r_3^2) & & \\
&\theta_{1s} = \tfrac{3}{2}c_3(x_1y_1-x_1y_3+y_1x_3) & &\theta_{1c} = -\tfrac{3}{4}c_3(x_1^2-y_1^2)+\tfrac{3}{2}c_3(x_1x_3+y_1y_3) \\
&\theta_{2s} = \tfrac{3}{2}c_3(x_1y_3+y_1x_3) & &\theta_{2c} = \tfrac{3}{2}c_3(-x_1x_3+y_1y_3) \\
&\theta_{3s} = \tfrac{3}{2}c_3x_3y_3 & &\theta_{3c} = -\tfrac{3}{4}c_3(x_3^2-y_3^2)
\end{aligned} \tag{1.16$_1$}$$

By Floquet's theorem [12], the general solution of Eq. (1.16) takes the form

$$\eta(\tau) = Ae^{\mu\tau}\phi(\tau)+Be^{-\mu\tau}\psi(\tau) \tag{1.17}$$

where A and B are arbitrary constants, $\phi(\tau)$ and $\psi(\tau)$ are periodic functions of τ of period π or 2π, and μ is the characteristic exponent to be determined by the parameters θ's and may be considered to be real or imaginary, but not complex. From the theory of Hill's equation [14, 18, 30] we see that there are regions of parameters θ's in which the solution, Eq. (1.17), is either stable (μ: imaginary) or unstable (μ: real), and that these regions of stability and instability appear alternately as parameter θ_0 increases. For convenience, we shall call the regions of instability as the first, the second, $\cdots$, unstable regions as parameter θ_0 increases from zero. It is known that the periodic functions $\phi(\tau)$ and $\psi(\tau)$ in Eq. (1.17) are composed of odd-order harmonics in the regions of odd orders and even-order harmonics in the regions of even orders and that, in the nth unstable region, the nth harmonic component predominates over other harmonics.

Since Eq. (1.7) is an approximate solution of Eq. (1.6), a solution of Eq. (1.16) may reasonably be an approximation of the same order. Therefore we assume that a particular solution in the first and the third unstable regions is given by

$$\eta(\tau) = e^{\mu\tau}\phi(\tau) = e^{\mu\tau}[b_1\sin(\tau-\sigma_1)+b_3\sin(3\tau-\sigma_3)] \tag{1.18}$$

We substitute this into Eq. (1.16) and apply the method of harmonic balance to obtain

$$\Delta_1(\mu)\equiv\begin{vmatrix}
\theta_0+\mu^2-1-\theta_{1c} & \theta_{1s}-2\mu & \theta_{1c}-\theta_{2c} & -\theta_{1s}+\theta_{2s} \\
\theta_{1s}+2\mu & \theta_0+\mu^2-1+\theta_{1c} & \theta_{1s}+\theta_{2s} & \theta_{1c}+\theta_{2c} \\
\theta_{1c}-\theta_{2c} & \theta_{1s}+\theta_{2s} & \theta_0+\mu^2-9-\theta_{3c} & \theta_{3s}-6\mu \\
-\theta_{1s}+\theta_{2s} & \theta_{1c}+\theta_{2c} & \theta_{3s}+6\mu & \theta_0+\mu^2-9+\theta_{3c}
\end{vmatrix} = 0 \tag{1.19}$$

From Eqs. (1.14) and (1.17) we see that the variation ξ tends to zero with increasing

τ provided that $|\mu|<\delta$. Hence the stability condition for the first and the third unstable regions is given by

$$\Delta_1(\delta)>0 \tag{1.20}$$

By virtue of Eqs. (1.8) and (1.16_1), the stability condition (1.20) leads to

$$\Delta_1(\delta)\equiv\begin{vmatrix} \frac{\partial X_1}{\partial x_1} & \frac{\partial X_1}{\partial y_1} & \frac{\partial X_1}{\partial x_3} & \frac{\partial X_1}{\partial y_3} \\ \frac{\partial Y_1}{\partial x_1} & \frac{\partial Y_1}{\partial y_1} & \frac{\partial Y_1}{\partial x_3} & \frac{\partial Y_1}{\partial y_3} \\ \frac{\partial X_3}{\partial x_1} & \frac{\partial X_3}{\partial y_1} & \frac{\partial X_3}{\partial x_3} & \frac{\partial X_3}{\partial y_3} \\ \frac{\partial Y_3}{\partial x_1} & \frac{\partial Y_3}{\partial y_1} & \frac{\partial Y_3}{\partial x_3} & \frac{\partial Y_3}{\partial y_3} \end{vmatrix}\equiv\frac{\partial(X_1, Y_1, X_3, Y_3)}{\partial(x_1, y_1, x_3, y_3)}>0 \tag{1.21}$$

Differentiating Eqs. (1.8) with respect to B yields

$$\begin{aligned} \frac{\partial X_1}{\partial x_1}\frac{dx_1}{dB}+\frac{\partial X_1}{\partial y_1}\frac{dy_1}{dB}+\frac{\partial X_1}{\partial x_3}\frac{dx_3}{dB}+\frac{\partial X_1}{\partial y_3}\frac{dy_3}{dB}&=0 \\ \frac{\partial Y_1}{\partial x_1}\frac{dx_1}{dB}+\frac{\partial Y_1}{\partial y_1}\frac{dy_1}{dB}+\frac{\partial Y_1}{\partial x_3}\frac{dx_3}{dB}+\frac{\partial Y_1}{\partial y_3}\frac{dy_3}{dB}&=1 \\ \frac{\partial X_3}{\partial x_1}\frac{dx_1}{dB}+\frac{\partial X_3}{\partial y_1}\frac{dy_1}{dB}+\frac{\partial X_3}{\partial x_3}\frac{dx_3}{dB}+\frac{\partial X_3}{\partial y_3}\frac{dy_3}{dB}&=0 \\ \frac{\partial Y_3}{\partial x_1}\frac{dx_1}{dB}+\frac{\partial Y_3}{\partial y_1}\frac{dy_1}{dB}+\frac{\partial Y_3}{\partial x_3}\frac{dx_3}{dB}+\frac{\partial Y_3}{\partial y_3}\frac{dy_3}{dB}&=0 \end{aligned} \tag{1.22}$$

Solving these simultaneous equations gives

$$\frac{dx_1}{dB}=\frac{\Delta_{21}}{\Delta} \qquad \frac{dy_1}{dB}=\frac{\Delta_{22}}{\Delta} \qquad \frac{dx_3}{dB}=\frac{\Delta_{23}}{\Delta} \qquad \frac{dy_3}{dB}=\frac{\Delta_{24}}{\Delta} \tag{1.23}$$

where Δ_{2i} $(i=1\sim 4)$ is the cofactor of row 2 and column i of the determinant $\Delta(\equiv\Delta_1(\delta))$. Consequently we have

$$\frac{dr_1}{dB}=\frac{1}{r_1\Delta}(x_1\Delta_{21}+y_1\Delta_{22}) \qquad \frac{dr_3}{dB}=\frac{1}{r_3\Delta}(x_3\Delta_{23}+y_3\Delta_{24}) \tag{1.24}$$

where $\quad r_1^2=x_1^2+y_1^2 \qquad r_3^2=x_3^2+y_3^2$

Hence the vertical tangency of the characteristic curves (Br_1 and Br_3 relations) occurs at the stability limit $\Delta=0$ of the first and the third unstable regions.

A particular solution of Eq. (1.16) in the second unstable region may preferably be written as

$$\eta(\tau)=e^{\mu\tau}\phi(\tau)=e^{\mu\tau}[b_0+b_2\sin(2\tau-\sigma_2)] \tag{1.25}$$

Proceeding analogously as above, the characteristic exponent μ is determined by

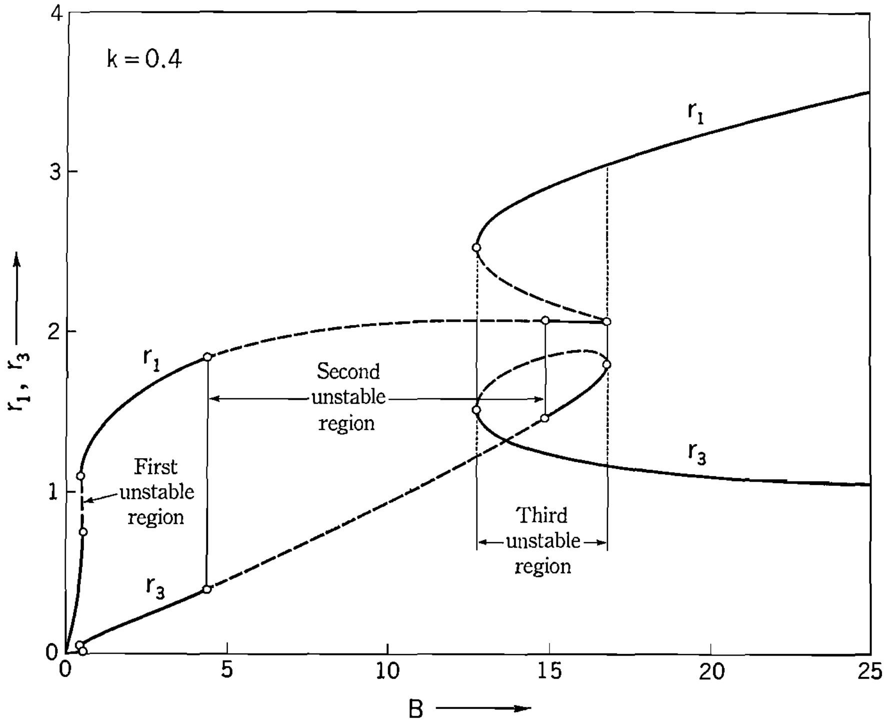

FIG. 1.2 Amplitude characteristic of the periodic solution given by Eq. (1.7).

$$\Delta_2(\mu) \equiv \begin{vmatrix} \theta_0+\mu^2 & \theta_{1s} & \theta_{1c} \\ 2\theta_{1s} & \theta_0+\mu^2-4-\theta_{2c} & \theta_{2s}-4\mu \\ 2\theta_{1c} & \theta_{2s}+4\mu & \theta_0+\mu^2-4+\theta_{2c} \end{vmatrix} = 0 \tag{1.26}$$

and the stability condition for the second unstable region, i.e., $|\mu| < \delta$, is given by

$$\Delta_2(\delta) > 0 \tag{1.27}$$

NUMERICAL EXAMPLE

Putting $k = 0.4$, $c_1 = 0$, and $c_3 = 1$ in Eq. (1.6) gives

$$\frac{d^2v}{d\tau^2} + 0.4\frac{dv}{d\tau} + v^3 = B \cos \tau$$

By use of Eqs. (1.9) the amplitude characteristics of Eq. (1.7) were calculated for this particular case and plotted against B in Fig. 1.2. The dotted portions of the characteristic curves represent unstable states, since the stability condition (1.20) or (1.27) is not satisfied in these intervals.

(*c*) *Periodic Solution Containing Even-order Harmonics Also and Its Stability*

It has been pointed out in Sec. 1.3*b* that even-order harmonics are self-excited in the second unstable region (see Fig. 1.2). In this region, the self-excited oscillation would gradually build up with increasing amplitude taking the form

$$e^{(\mu-\delta)\tau}[b_0+b_2 \sin (2\tau-\sigma_2)] \quad \text{with} \quad \mu-\delta>0$$

and ultimately get to the steady state with a constant amplitude which is limited by the nonlinearity of the system. This implies that, under certain intervals of B, such even-order harmonics must be considered in the periodic solution. Therefore we assume a periodic solution for Eq. (1.6) of the form

$$v_0(\tau) = z+x_1 \sin \tau+y_1 \cos \tau+x_2 \sin 2\tau+y_2 \cos 2\tau \tag{1.28}$$

Terms of harmonics higher than the second, especially the third harmonic, are certain to be present but are ignored to avoid unwieldy calculations. The unknown coefficients in the right side of Eq. (1.28) are determined in much the same manner as before; that is, substituting Eq. (1.28) into (1.6) and equating the coefficients of the nonoscillatory term and of the terms containing $\sin \tau$, $\cos \tau$, $\sin 2\tau$, and $\cos 2\tau$ separately to zero yields

$$\begin{aligned}
-A_0 z+\tfrac{3}{4}c_3[2x_1y_1x_2-(x_1^2-y_1^2)y_2] &\equiv Z(z, x_1, y_1, x_2, y_2) = 0\\
-A_1x_1-ky_1+3c_3z(y_1x_2-x_1y_2) &\equiv X_1(z, x_1, y_1, x_2, y_2) = 0\\
kx_1-A_1y_1+3c_3z(x_1x_2+y_1y_2) &\equiv Y_1(z, x_1, y_1, x_2, y_2) = B\\
-A_2x_2-2ky_2+3c_3zx_1y_1 &\equiv X_2(z, x_1, y_1, x_2, y_2) = 0\\
2kx_2-A_2y_2-\tfrac{3}{2}c_3z(x_1^2-y_1^2) &\equiv Y_2(z, x_1, y_1, x_2, y_2) = 0
\end{aligned} \tag{1.29}$$

where
$$\begin{aligned}
A_0 &= -c_1-c_3[z^2+\tfrac{3}{2}(r_1^2+r_2^2)]\\
A_1 &= 1-c_1-\tfrac{3}{4}c_3(4z^2+r_1^2+2r_2^2) \qquad A_2 = 4-c_1-\tfrac{3}{4}c_3(4z^2+2r_1^2+r_2^2)\\
r_1^2 &= x_1^2+y_1^2 \qquad\qquad r_2^2 = x_2^2+y_2^2
\end{aligned}$$

Elimination of the x and y components in the above equations gives

$$\begin{gathered}
\left[\left(A_1-\frac{2r_2^2}{r_1^2}A_2\right)^2+k^2\left(1+\frac{4r_2^2}{r_1^2}\right)^2\right]r_1^2 = B^2\\
-A_0z^2+\tfrac{1}{2}A_2r_2^2 = 0\\
(A_2^2+4k^2)r_2^2 = \tfrac{9}{4}c_3^2z^2r_1^4
\end{gathered} \tag{1.30}$$

From these relations z, r_1, and r_2 are determined. By use of Eqs. (1.29) and (1.30) the coefficients of the periodic solution are found to be

$$x_1 = \frac{k(r_1^2+4r_2^2)}{B} \qquad y_1 = \frac{-(A_1r_1^2-2A_2r_2^2)}{B} \tag{1.31}$$

and
$$x_2 = \frac{4r_2^2}{3c_3zr_1^4}[A_2x_1y_1+k(x_1^2-y_1^2)] \qquad y_2 = \frac{4r_2^2}{3c_3zr_1^4}[2kx_1y_1-\tfrac{1}{2}A_2(x_1^2-y_1^2)] \tag{1.32}$$

Proceeding analogously as in Sec. 1.3*b*, the condition for stability may also be derived; namely, inserting $v_0(\tau)$ as given by Eq. (1.28) into (1.15) leads to a Hill's equation of the form

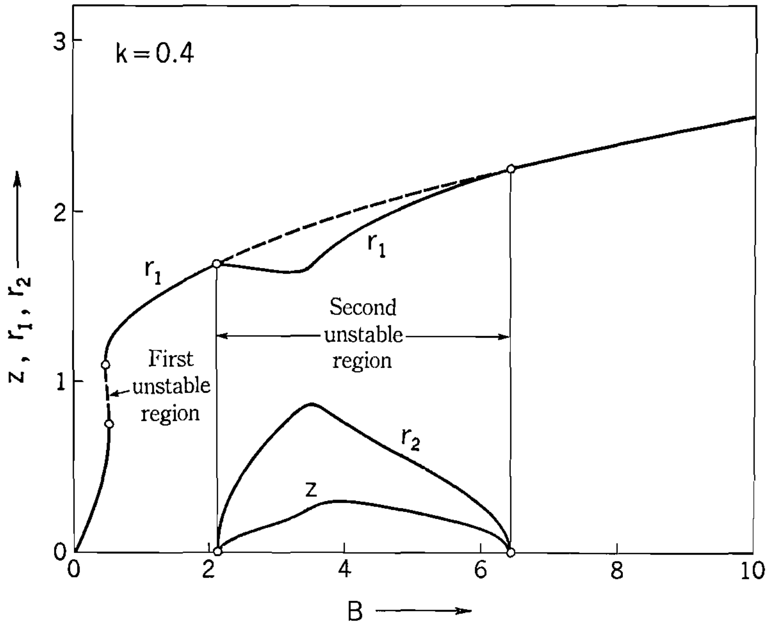

FIG. 1.3 Amplitude characteristic of the periodic solution given by Eq. (1.28).

$$\frac{d^2\eta}{d\tau^2}+\left(\theta_0+2\sum_{n=1}^{4}\theta_{ns}\sin n\tau+2\sum_{n=1}^{4}\theta_{nc}\cos n\tau\right)\eta=0 \tag{1.33}$$

where

$$\xi\,(=v-v_0)=e^{-\delta\tau}\cdot\eta$$

A particular solution of Eq. (1.33) in the second unstable region may be assumed as

$$\eta(\tau)=e^{\mu\tau}\phi(\tau)=e^{\mu\tau}[b_0+b_1\sin(\tau-\sigma_1)+b_2\sin(2\tau-\sigma_2)] \tag{1.34}$$

By use of Eqs. (1.29) the stability condition is obtained as*

$$\frac{\partial(Z, X_1, Y_1, X_2, Y_2)}{\partial(z, x_1, y_1, x_2, y_2)}>0 \tag{1.35}$$

NUMERICAL EXAMPLE

By use of Eqs. (1.30) the amplitude characteristics of Eq. (1.28) were calculated and plotted in Fig. 1.3. The system parameters are the same as in Fig. 1.2, i.e., $k=0.4$, $c_1=0$, and $c_3=1$. The dotted portions represent unstable state since condition (1.35) is not satisfied. It is to be noted that the second unstable region of Fig. 1.3 is narrower than that of Fig. 1.2 because the third harmonic in Eq. (1.28) was

* As the coefficient of η in Eq. (1.33) contains even and odd harmonics, there are regions of parameters θ's in which the 1/2, 3/2, $\cdots$, harmonics are excited. This implies that in the second unstable region of Fig. 1.3 there may exist intervals of B such that 1/2, 3/2, $\cdots$, harmonics develop. A detailed investigation of such a case is, however, omitted here (cf. Secs. 1.5c and 1.6).

neglected. It is worth mentioning that the second harmonic is sustained in the second unstable region even though the system is symmetrical.

1.4 Analog-computer Analysis

The results obtained in the preceding sections will be compared with the solutions obtained by using an analog computer. The block diagram of Fig. 1.4 shows an analog-computer setup for the solution of Eq. (1.6), in which the system parameters k, c_1, and c_3 are set equal to the values as given in Secs. 1.3*b* and *c*; i.e.,

$$\frac{d^2v}{d\tau^2}+0.4\frac{dv}{d\tau}+v^3 = B\cos\tau \qquad (1.36)$$

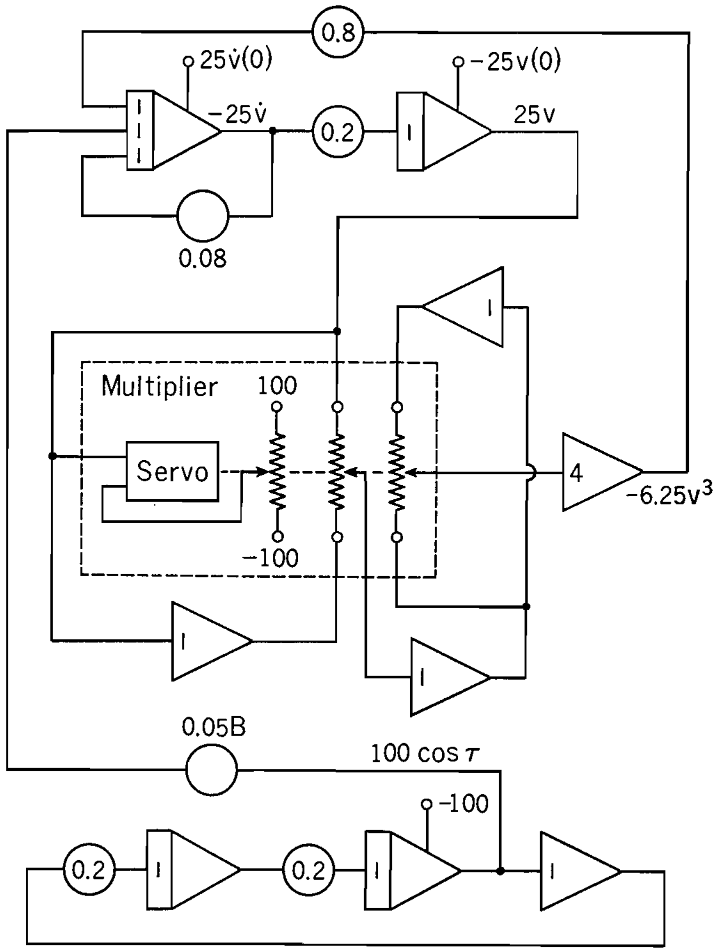

FIG. 1.4 Block diagram of an analog-computer setup for the solution of Eq. (1.36).

The symbols in the figure follow the conventional notation.* The solutions of Eq. (1.36) are sought for various values of B, the amplitude of the external force. From the solutions obtained in this way, we see that the first unstable region ranges from $B=0.45$ to 0.53. The second unstable region extends from $B=2.7$ to 12.6. In this region the concurrence of the $1/2$, $3/2$, $\cdots$, harmonic components is confirmed in the intervals of B approximately from 7 to 11. The third unstable region occurs between $B=12.6$ and 14.9.

1.5 Solution of the Fundamental Equation Using Mapping Concepts

This section describes the mapping method based on the transformation theory of nonlinear differential equations [3, 17] and gives some numerical results of the solution of Duffing's equation.

(a) Mapping and Fixed Points

In studying periodic solutions of Eq. (1.6) it is helpful to use the phase plane, with coordinates v and $\dot{v}(=dv/d\tau)$. Equation (1.6) then becomes the system

$$\begin{aligned}\frac{dv}{d\tau}&=\dot{v}\\ \frac{d\dot{v}}{d\tau}&=-k\dot{v}-c_1v-c_3v^3+B\cos\tau\end{aligned}\tag{1.37}$$

We see that the right sides are analytic in v, $\dot{v}$, and τ, and are periodic in τ with period 2π.

It is well known that to a system such as Eqs. (1.37) there corresponds a mapping of the $v\dot{v}$ plane into itself. To see this let us consider the solution $(v(v_0, \dot{v}_0, \tau)$, $\dot{v}(v_0, \dot{v}_0, \tau))$ of Eqs. (1.37) which when $\tau=0$ is at the point $(v_0, \dot{v}_0)$ of $v\dot{v}$ plane. Let

$$v_n=v(v_0, \dot{v}_0, 2n\pi) \qquad \dot{v}_n=\dot{v}(v_0, \dot{v}_0, 2n\pi)\tag{1.38}$$

for any integer n. Since the right sides of Eqs. (1.37) are of period 2π in τ, it follows that

$$v_{n+m}=v(v_m, \dot{v}_m, 2n\pi) \qquad \dot{v}_{n+m}=\dot{v}(v_m, \dot{v}_m, 2n\pi)\tag{1.39}$$

Let P_n denote the point $(v_n, \dot{v}_n)$, then we define a topological mapping T of the $v\dot{v}$ plane into itself by $P_1=TP_0$.** By T^n is meant the mapping that takes P_0 into P_n. Clearly Eqs. (1.39) are equivalent to $T^{n+m}P_0=T^nP_m=T^nT^mP_0$.

Now if $(v(v_0, \dot{v}_0, \tau)$, $\dot{v}(v_0, \dot{v}_0, \tau))$ has period 2π, then $P_1=P_0$, so that the point P_0 is a fixed point of the mapping T. In particular a fixed point under the mapping

* The integrating amplifiers in the block diagram integrate their inputs with respect to the machine time (in second), which is, in this particular case, 5 times the independent variable τ.

** This follows from well-known properties (the existence and uniqueness of solutions and the dependence of solutions on initial conditions) of solutions of Eqs. (1.37) [8, 27].

$T^{\nu}(\nu=2, 3, \cdots)$ corresponds to a periodic solution for Eqs. (1.37) of least period $2\nu\pi$, i.e., a subharmonic of order ν.

(*b*) *Stability of Fixed Points*

Let us study the mapping T in the neighborhood of a fixed point of the mapping. This will be facilitated by making a transformation of coordinates which takes the fixed point into the origin. That is let $(v_0(\tau), \dot{v}_0(\tau))$ be a solution of Eqs. (1.37) of period $2\nu\pi(\nu=1, 2, 3, \cdots)$. Then the point $(v_0(0), \dot{v}_0(0))$ is a fixed point under T^{ν}. Let P_0 be the point $(v_0(0)+u_0, \dot{v}_0(0)+\dot{u}_0)$ in the $v\dot{v}$ plane. Denote $T^{\nu}P_0$ by P_ν with coordinates $(v_0(0)+u_\nu, \dot{v}_0(0)+\dot{u}_\nu)$, then the u_ν and $\dot{u}_\nu$ can be expressed by power series in u_0 and $\dot{u}_0$; that is

$$\begin{aligned} u_\nu &= au_0+b\dot{u}_0+\cdots \\ \dot{u}_\nu &= cu_0+d\dot{u}_0+\cdots \end{aligned} \tag{1.40}$$

with

$$a=\left(\frac{\partial v(\xi, \eta, 2\nu\pi)}{\partial \xi}\right)_0 \qquad b=\left(\frac{\partial v(\xi, \eta, 2\nu\pi)}{\partial \eta}\right)_0$$

$$c=\left(\frac{\partial \dot{v}(\xi, \eta, 2\nu\pi)}{\partial \xi}\right)_0 \qquad d=\left(\frac{\partial \dot{v}(\xi, \eta, 2\nu\pi)}{\partial \eta}\right)_0$$

where $\left(\frac{\partial v}{\partial \xi}\right)_0, \cdots, \left(\frac{\partial \dot{v}}{\partial \eta}\right)_0$ denote the values of $\frac{\partial v}{\partial \xi}, \cdots, \frac{\partial \dot{v}}{\partial \eta}$ at $\xi=v_0(0)$ and $\eta=\dot{v}_0(0)$, respectively, and the terms not explicitly given in the right sides are of degree two or higher in u_0 and $\dot{u}_0$. For small values of u_0 and $\dot{u}_0$, the character of the mapping (1.40) is determined by its linear terms. That is, the mapping can be characterized by the roots of the equation

$$\begin{vmatrix} a-\rho & b \\ c & d-\rho \end{vmatrix} = 0 \tag{1.41}$$

A fixed point is called simple if the absolute values of the corresponding characteristic roots, ρ_1 and ρ_2, are both different from unity. Using terminology in Levinson's paper [17], we classify simple fixed points of the mapping in the following form*

Completely stable if	$\lvert\rho_1\rvert<1$ and $\lvert\rho_2\rvert<1$
Completely unstable if	$\lvert\rho_1\rvert>1$ and $\lvert\rho_2\rvert>1$
Directly unstable if	$0<\rho_1<1<\rho_2$
Inversely unstable if	$\rho_1<-1<\rho_2<0$

If a fixed point is completely stable, there is a neighborhood of a fixed point such that all points in this neighborhood tend to the fixed point under repeated applications of the mapping. In the completely unstable case, we have the situation of points moving away from the fixed point under the mapping. In the directly or

* We will see later in Eq. (1.44) that the product $\rho_1\rho_2$ is always positive.

inversely unstable case, most but not all points will move away from the fixed point.

It is worth mentioning that Eq. (1.41) coincides with the characteristic equation of the variational system for the periodic solution $(v_0(\tau), \dot{v}_0(\tau))$. Let $(\xi(\tau), \eta(\tau))$ be a samll variation from a periodic solution $(v_0(\tau), \dot{v}_0(\tau))$ defined by

$$v(\tau) = v_0(\tau)+\xi(\tau) \qquad \dot{v}(\tau) = \dot{v}_0(\tau)+\eta(\tau)$$

Then, the variational system is

$$\begin{aligned} \frac{d\xi}{d\tau} &= \eta \\ \frac{d\eta}{d\tau} &= -(c_1+3c_3v_0^2(\tau))\xi-k\eta \end{aligned} \tag{1.42}$$

Since $v_0(\tau)$ is periodic, Eqs. (1.42) are linear differential equations with periodic coefficients. Let $(\xi_i(\tau), \eta_i(\tau))$ $(i=1, 2)$ be the fundamental set of solutions of Eqs. (1.42) with the initial conditions

$$\begin{aligned} \xi_1(0) &= 1 \qquad & \xi_2(0) &= 0 \\ \eta_1(0) &= 0 \qquad & \eta_2(0) &= 1 \end{aligned}$$

Then the characteristic equation for Eqs. (1.42) corresponding to the period $2\nu\pi$ is given by [19]*

$$\begin{vmatrix} \xi_1(2\nu\pi)-\rho & \xi_2(2\nu\pi) \\ \eta_1(2\nu\pi) & \eta_2(2\nu\pi)-\rho \end{vmatrix} = 0 \tag{1.43}$$

The roots of the above equation are sometimes called the characteristic multipliers of the variational system (1.42). From the theory of linear equations with periodic coefficients, the product of the roots of Eq. (1.43) is given by

$$\rho_1\rho_2 = \begin{vmatrix} \xi_1(2\nu\pi) & \xi_2(2\nu\pi) \\ \eta_1(2\nu\pi) & \eta_2(2\nu\pi) \end{vmatrix} = \exp(-2\nu\pi k) > 0 \tag{1.44}$$

(*c*) *Numerical Analysis*

We will here give some examples of fixed points and corresponding periodic solutions of Eqs. (1.37) using the mapping method. The successive images P_n $(v(2n\pi), \dot{v}(2n\pi))$ $(n=1, 2, 3,\cdots)$ of the initial point $P_0(v(0), \dot{v}(0))$ under the mapping T are actually obtained by using computer facilities. The numerical integration, using the Runge-Kutta-Gill's method, was carried out on the KDC-I Digital Computer. If an initial point P_0 is chosen sufficiently near a completely stable fixed point, the point sequence $\{P_n\}$ converges to the fixed point as $n\to\infty$. In order to locate a completely stable fixed point, we first determine the initial point P_0 by making use of the results obtained in the preceding sections. Then, the

* The magnitudes $\xi_1(2\nu\pi)$, $\xi_2(2\nu\pi)$, $\eta_1(2\nu\pi)$, and $\eta_2(2\nu\pi)$ are equal to the coefficients a, b, c, and d in Eqs. (1.41), respectively.

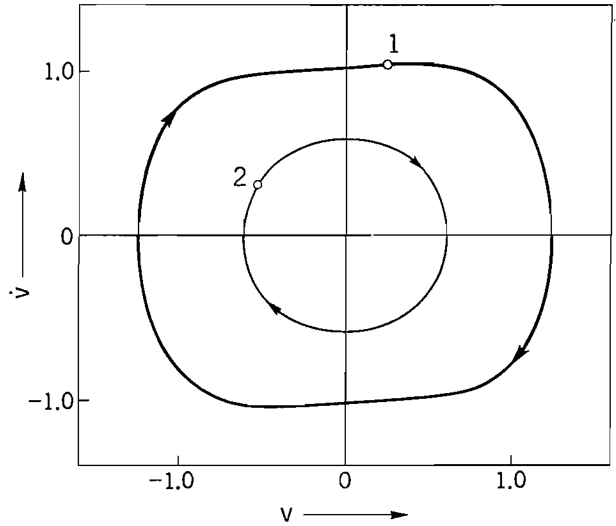

FIG. 1.5 Fixed points and trajectories of the stable solutions for Eq. (1.46).

successive images are calculated until the following condition is satisfied*

$$|P_n - P_{n+\nu}| < \varepsilon$$

where ε is a small positive constant, $\nu=1$ for harmonic responses, and $\nu=2, 3, \cdots$ for subharmonic responses of order ν. Once the fixed point is determined, the corresponding trajectory and periodic solution are easily obtained. Because of the nature of this procedure, only the stable solutions are discussed.

Examples of the periodic solutions and their trajectories of Eq. (1.6) are given below for the system parameters $k=0.4$, $c_1=0$, and $c_3=1$

$$\frac{d^2v}{d\tau^2}+0.4\frac{dv}{d\tau}+v^3 = B\cos\tau \tag{1.45}$$

CASE 1. WHEN THE AMPLITUDE B OF THE EXTERNAL FORCE LIES IN THE FIRST UNSTABLE REGION

We consider the equation

$$\frac{d^2v}{d\tau^2}+0.4\frac{dv}{d\tau}+v^3 = 0.5\cos\tau \tag{1.46}$$

For this particular value of B, there are two completely stable fixed points, 1 and 2. Figure 1.5 shows the locations of the fixed points and the correlated trajectories. The periodic solutions, $v_{01}(\tau)$ and $v_{02}(\tau)$, correlated with points 1 and 2, respectively, are given by

* The value of ε is taken equal to 10^{-5} in the following examples.

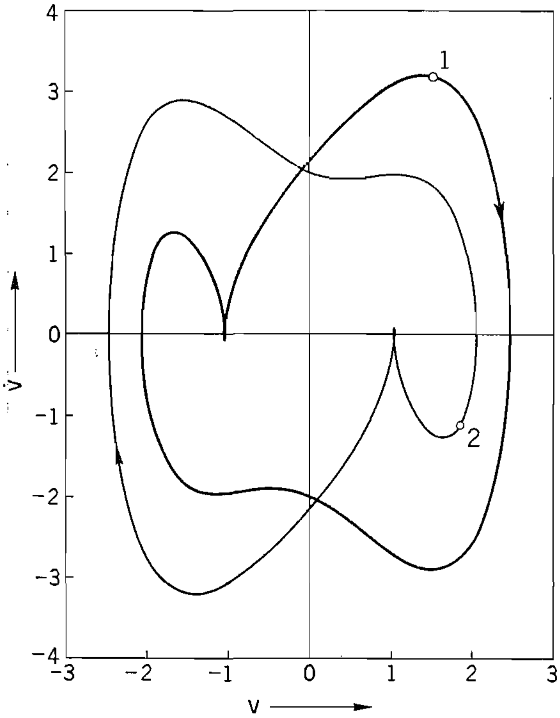

FIG. 1.6 Fixed points and trajectories of the stable solutions for Eq. (1.49).

$$v_{01}(\tau) = 1.14 \sin \tau + 0.30 \cos \tau - 0.04 \sin 3\tau - 0.05 \cos 3\tau \tag{1.47}$$

$$v_{02}(\tau) = 0.29 \sin \tau - 0.53 \cos \tau + 0.01 \sin 3\tau + 0.00 \cos 3\tau \tag{1.48}$$

CASE 2. WHEN THE AMPLITUDE B OF THE EXTERNAL FORCE LIES IN THE SECOND UNSTABLE REGION

We consider the case in which B is given in the second unstable region and Eq. (1.45) becomes

$$\frac{d^2v}{d\tau^2} + 0.4\frac{dv}{d\tau} + v^3 = 4 \cos \tau \tag{1.49}$$

There are two completely stable fixed points, 1 and 2. These fixed points and the correlated trajectories are shown in Fig. 1.6. Corresponding to points 1 and 2 we have

$$\begin{aligned} v_{01}(\tau) &= -v_{02}(\tau - \pi) \\ &= -0.31 + 0.60 \sin \tau + 1.59 \cos \tau + 0.73 \sin 2\tau + 0.20 \cos 2\tau \\ &\quad + 0.11 \sin 3\tau + 0.15 \cos 3\tau + 0.15 \sin 4\tau - 0.04 \cos 4\tau \\ &\quad + 0.02 \sin 5\tau - 0.03 \cos 5\tau + 0.02 \sin 6\tau - 0.02 \cos 6\tau \\ &\quad - 0.00 \sin 7\tau - 0.01 \cos 7\tau \end{aligned} \tag{1.50}$$

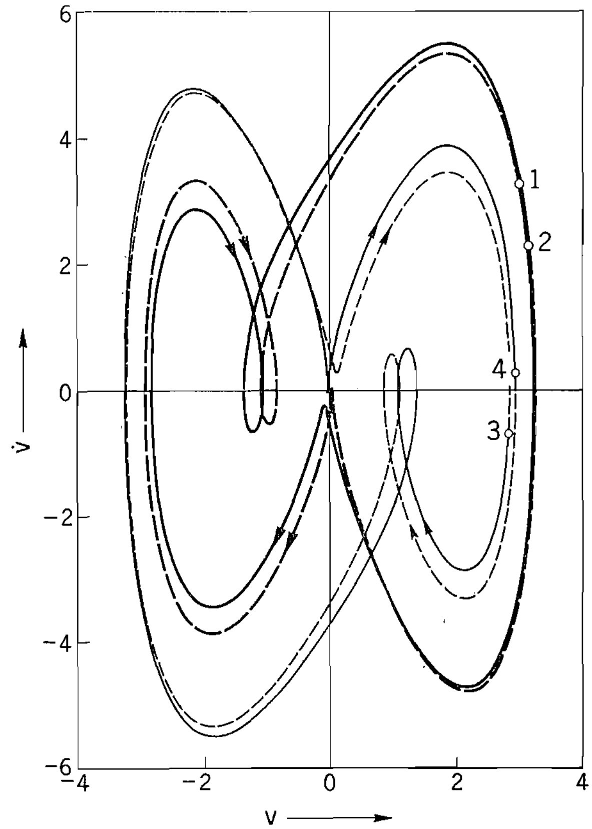

FIG. 1.7 Fixed points and trajectories of the stable solutions for Eq. (1.51).

Next we consider the case in which B is increased and the equation becomes

$$\frac{d^2v}{d\tau^2}+0.4\frac{dv}{d\tau}+v^3 = 9 \cos \tau \tag{1.51}$$

In this case there are four completely stable fixed points, 1, 2, 3, and 4. Each of them is obtained under every second iteration of the mapping T, i.e., under the mapping T^2. Their locations and the trajectories are shown in Fig. 1.7. It is to be noted that points 1 and 2 (or 3 and 4) lie on the same trajectory and under the mapping T, point 1 (or 3) moves to point 2 (or 4) and point 2 (or 4) to point 1 (or 3). In order to distinguish clearly the trajectory from point 1 to 2 (or 3 to 4) from that from point 2 to 1 (or 4 to 3), the former is shown by full line and the latter by dotted line. The periodic solutions correlated with these fixed points are given by

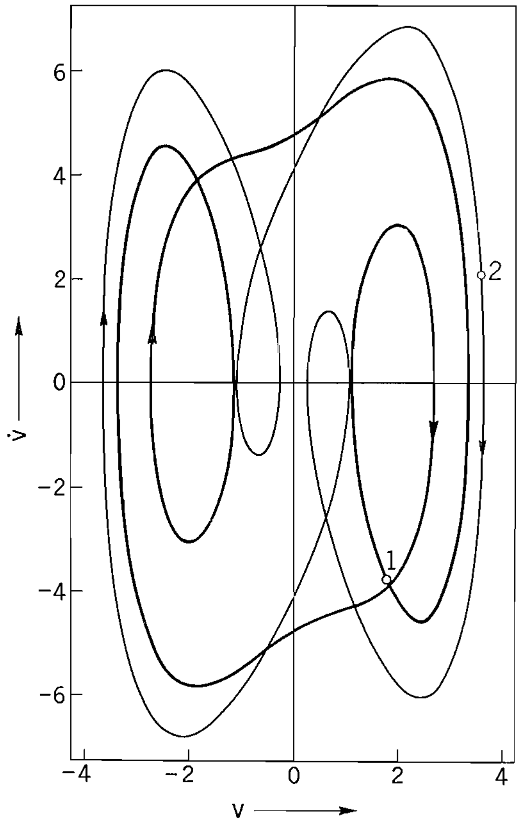

FIG. 1.8 Fixed points and trajectories of the stable solutions for Eq. (1.53).

$$
\begin{aligned}
v_{01}(\tau) &= v_{02}(\tau-2\pi) = -v_{03}(\tau-\pi) = -v_{04}(\tau-3\pi) \\
&= -0.31-0.06 \sin \tfrac{1}{2}\tau \; +0.01 \cos \tfrac{1}{2}\tau \; +0.58 \sin \tau \; +1.84 \cos \tau \\
&\quad -0.00 \sin \tfrac{3}{2}\tau \; +0.01 \cos \tfrac{3}{2}\tau \; +0.26 \sin 2\tau+0.34 \cos 2\tau \\
&\quad +0.10 \sin \tfrac{5}{2}\tau \; -0.07 \cos \tfrac{5}{2}\tau \; +0.04 \sin 3\tau+0.89 \cos 3\tau \\
&\quad +0.01 \sin \tfrac{7}{2}\tau \; +0.02 \cos \tfrac{7}{2}\tau \; +0.11 \sin 4\tau+0.05 \cos 4\tau \\
&\quad +0.03 \sin \tfrac{9}{2}\tau \; -0.03 \cos \tfrac{9}{2}\tau \; +0.06 \sin 5\tau+0.18 \cos 5\tau \\
&\quad +0.00 \sin \tfrac{11}{2}\tau+0.00 \cos \tfrac{11}{2}\tau+0.05 \sin 6\tau+0.02 \cos 6\tau \\
&\quad +0.01 \sin \tfrac{13}{2}\tau-0.01 \cos \tfrac{13}{2}\tau+0.02 \sin 7\tau+0.05 \cos 7\tau \\
&\quad +0.00 \sin \tfrac{15}{2}\tau-0.00 \cos \tfrac{15}{2}\tau+0.02 \sin 8\tau+0.00 \cos 8\tau \\
&\quad +\cdots
\end{aligned}
\tag{1.52}
$$

CASE 3. WHEN THE AMPLITUDE B OF THE EXTERNAL FORCE LIES IN THE THIRD UNSTABLE REGION

Putting $B=13$ in Eq. (1.45) gives

$$
\frac{d^2v}{d\tau^2}+0.4\frac{dv}{d\tau}+v^3 = 13 \cos \tau \tag{1.53}
$$

In this case there are two completely stable fixed points, 1 and 2. Their locations and the correlated trajectories are shown in Fig. 1.8. Corresponding periodic solutions $v_{01}(\tau)$ and $v_{02}(\tau)$ are given by

$$\begin{aligned} v_{01}(\tau) = {} & 0.77 \sin \tau + 2.48 \cos \tau - 1.21 \sin 3\tau - 0.51 \cos 3\tau \\ & - 0.28 \sin 5\tau - 0.08 \cos 5\tau + 0.05 \sin 7\tau - 0.09 \cos 7\tau \\ & + 0.02 \sin 9\tau - 0.02 \cos 9\tau + 0.01 \sin 11\tau + 0.01 \cos 11\tau \end{aligned} \tag{1.54}$$

$$\begin{aligned} v_{02}(\tau) = {} & 0.78 \sin \tau + 1.67 \cos \tau + 0.07 \sin 3\tau + 1.40 \cos 3\tau \\ & + 0.09 \sin 5\tau + 0.35 \cos 5\tau + 0.05 \sin 7\tau + 0.12 \cos 7\tau \\ & + 0.02 \sin 9\tau + 0.04 \cos 9\tau + 0.01 \sin 11\tau + 0.01 \cos 11\tau \end{aligned} \tag{1.55}$$

The details of the completely stable fixed points appearing in the above examples are summed up and listed in Table 1.1. There are also given the related characteristic multipliers and the time increments h which are employed for carrying out the numerical integration.

TABLE 1.1 Completely Stable Fixed Points and Related Properties in Figs. 1.5, 1.6, 1.7, and 1.8

Fixed Point	B	v_0	$\dot{v}_0$	$\rho_{1,2}$	h
Fig. 1.5 1	0.5	0.253	1.040	$0.154 \pm 0.239i$	$\pi/30$
2	〃	−0.529	0.313	$0.047 \pm 0.281i$	〃
Fig. 1.6 1	4	1.522	3.181	$0.169 \pm 0.229i$	$\pi/30$
2	〃	1.863	−1.107	〃	〃
Fig. 1.7 1	9	2.986	3.277	0.257, 0.026	$\pi/60$
2	〃	3.146	2.281	〃	〃
3	〃	2.819	−0.700	〃	〃
4	〃	2.931	0.268	〃	〃
Fig. 1.8 1	13	1.782	−3.747	$0.033 \pm 0.283i$	$\pi/60$
2	〃	3.593	2.091	$-0.077 \pm 0.274i$	〃

1.6 Experimental Result

An experiment using a series-resonance circuit as illustrated in Fig. 1.1 has been performed [13, pp. 132–133]. The result is as follows.

Since B is proportional to the amplitude E of the applied voltage, varying E will bring about the excitation of higher harmonic oscillations. This is observed in Fig. 1.9, in which the effective value of the oscillating current is plotted (in thick line) for a wide range of the applied voltage. By making use of a heterodyne harmonic analyzer, this current is analyzed into harmonic components. These are shown by fine lines, the numbers on which indicate the order of the harmonics. The first unstable region ranges between 24 and 40 volts of the applied voltage; the jump phenomenon in this region has been called the ferro-resonance. The second unstable region extends from 180 to 580 volts. The third unstable region occurs between 660 and 670 volts, exhibiting another jump in amplitude.

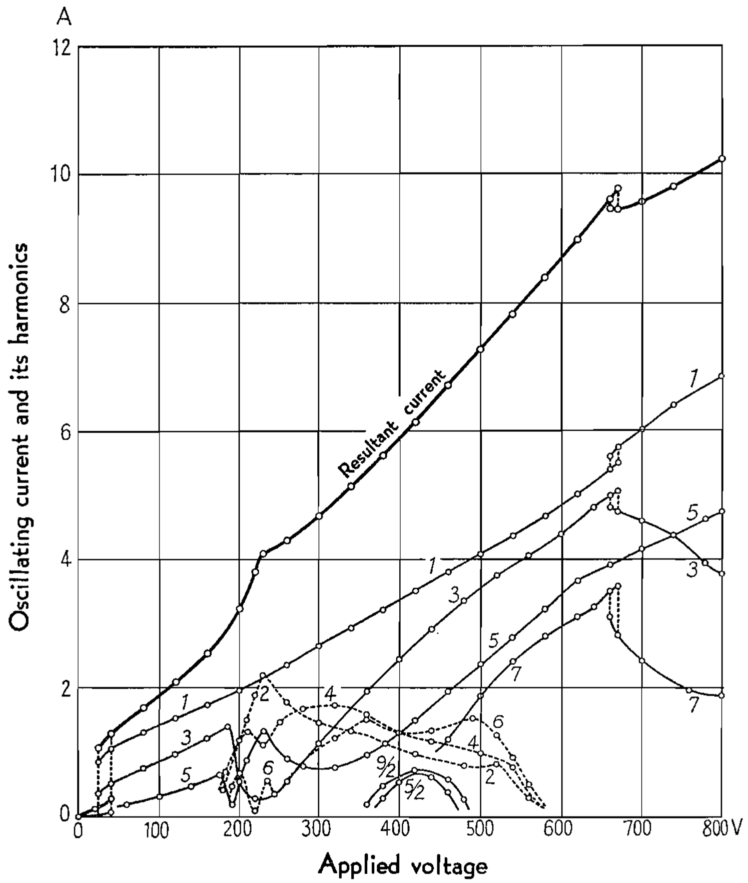

FIG. 1.9 Experimental result using a series-resonance circuit.

CHAPTER 2

HIGHER-HARMONIC OSCILLATIONS IN A PARALLEL-RESONANCE CIRCUIT

2.1 Introduction

In the preceding chapter, we investigated the higher-harmonic oscillations in a series-resonance circuit. Since the series condenser limits the current which magnetizes the reactor core, the applied voltage must be exceedingly raised in order to bring the oscillation into the unstable regions of higher order. On the other hand, we may expect that a higher harmonic oscillation is likely to occur in a parallel-resonance circuit because the reactor core is readily saturated under the impression of a comparatively low voltage; and this will be investigated in the present chapter. The differential equation which describes the system takes the form of Mathieu's equation with additional damping and nonlinear restoring terms. An experimental result is also cited at the end of this chapter.

2.2 Derivation of the Fundamental Equation

Figure 2.1 shows the schematic diagram of a parallel-resonance circuit, in which two oscillation circuits are connected in series, each having equal values of L, R, and C, respectively. With the notation of the figure, the equations for the circuit are written as

$$
\begin{aligned}
n\frac{d\phi_1}{dt} &= Ri_{R1} = \frac{1}{C}\int i_{C1}\,dt \\
n\frac{d\phi_2}{dt} &= Ri_{R2} = \frac{1}{C}\int i_{C2}\,dt
\end{aligned}
\qquad (2.1)
$$

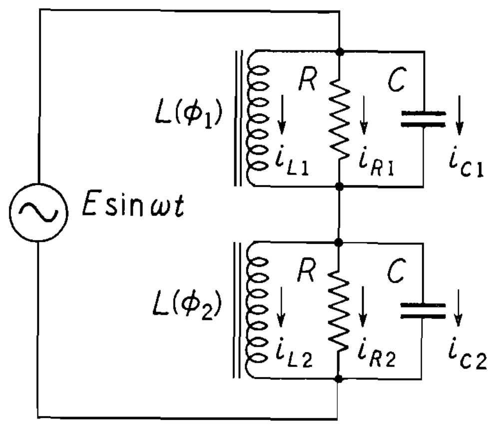

FIG. 2.1 Parallel-resonance circuit with nonlinear inductance.

$$n\frac{d\phi_1}{dt}+n\frac{d\phi_2}{dt} = E\sin\omega t$$

$$i = i_{L1}+i_{R1}+i_{C1} = i_{L2}+i_{R2}+i_{C2}$$

The same saturation curve is assumed for both of the inductors $L(\phi_1)$ and $L(\phi_2)$

$$i_{L1} = a_1\phi_1+a_3\phi_1^3 \qquad i_{L2} = a_1\phi_2+a_3\phi_2^3 \tag{2.2}$$

If the two oscillation circuits behave identically, we have, from the third member of Eqs. (2.1)

$$\phi_1 = \phi_2 = -\frac{E}{2n\omega}\cos\omega t$$

An increase of the flux ϕ_1 by ϕ results in the decrease of ϕ_2 by the same amount

$$\phi_1 = -\frac{E}{2n\omega}\cos\omega t+\phi \qquad \phi_2 = -\frac{E}{2n\omega}\cos\omega t-\phi \tag{2.3}$$

After elimination of i_{R1}, i_{R2}, i_{C1}, and i_{C2} in Eqs. (2.1) and by using Eqs. (2.3), we obtain

$$\frac{d^2\phi}{dt^2}+\frac{1}{CR}\frac{d\phi}{dt}+\frac{1}{2nC}(i_{L1}-i_{L2}) = 0 \tag{2.4}$$

Proceeding in the same manner as in Sec. 1.2, we introduce dimensionless variables defined by

$$i_{L1} = I\cdot u_{L1} \qquad i_{L2} = I\cdot u_{L2} \qquad \phi = \Phi\cdot v \tag{2.5}$$

and fix the base quantities, I and Φ by the following relations

$$n\omega^2C\Phi = I \qquad c_1+c_3 = 1 \tag{2.6}$$

where $$c_1 = \frac{a_1\Phi}{I} \qquad c_3 = \frac{a_3\Phi^3}{I}$$

Then, by use of Eqs. (2.2), (2.3), (2.5), and (2.6), Eq. (2.4) may be written in normalized from as

$$\frac{d^2v}{d\tau^2}+k\frac{dv}{d\tau}+\left(c_1+\frac{3}{2}c_3B^2+\frac{3}{2}c_3B^2\cos 2\tau\right)v+c_3v^3 = 0 \tag{2.7}$$

where $$\tau = \omega t \qquad k = \frac{1}{\omega CR} \qquad B = \frac{E}{2n\omega\Phi}$$

2.3 Solution of the Fundamental Equation Using Principle of Harmonic Balance

We assume for a moment that $k=0$ and v is so small that we may neglect the nonlinear term in Eq. (2.7). Then Eq. (2.7) reduces to a Mathieu's equation

$$\frac{d^2v}{d\tau^2}+(\theta_0+2\theta_1\cos 2\tau)v = 0 \tag{2.8}$$

where $$\theta_0 = c_1+\tfrac{3}{2}c_3B^2 \qquad \theta_1 = \tfrac{3}{4}c_3B^2$$

From the theory of Mathieu's equation [18, 20, 30] we see that there are regions of parameters, θ_0 and θ_1, in which the solution for Eq. (2.8) is either stable (remains bounded as τ increases) or unstable (diverges unboundedly), and that these regions of stability and instability appear alternately as parameter θ_0 increases. We shall call such regions of instability as the first, the second, $\cdots$, unstable regions as parameter θ_0 increases from zero. When the parameters θ_0 and θ_1 lie in the nth unstable region, a higher harmonic of the nth order is predominantly excited. Once the oscillation builds up, the nonlinear term c_3v^3 in Eq. (2.7) may not be ignored. It is this term that finally prevents the amplitude of the oscillation from growing up unboundedly.

(*a*) *Periodic Solutions*

After these preliminary remarks, we now proceed to investigate the periodic solution of Eq. (2.7) and assume the following form of the solution.

Harmonic: $$v_0(\tau) = x_1 \sin \tau + y_1 \cos \tau \tag{2.9}$$

Second-harmonic: $$v_0(\tau) = z + x_2 \sin 2\tau + y_2 \cos 2\tau \tag{2.10}$$

Third-harmonic: $$v_0(\tau) = x_1 \sin \tau + y_1 \cos \tau + x_3 \sin 3\tau + y_3 \cos 3\tau \tag{2.11}$$

(i) Harmonic Oscillation

In order to determine the coefficients in the right side of Eq. (2.9), we use the method of harmonic balance; namely, substituting Eq. (2.9) into (2.7) and equating the coefficients of the terms containing $\sin \tau$ and $\cos \tau$ separately to zero yields

$$\begin{aligned} -(A_1+\tfrac{3}{4}c_3B^2)x_1 - ky_1 &\equiv X_1(x_1, y_1) = 0 \\ kx_1 - (A_1-\tfrac{3}{4}c_3B^2)y_1 &\equiv Y_1(x_1, y_1) = 0 \end{aligned} \tag{2.12}$$

where $$A_1 = 1 - c_1 - \tfrac{3}{4}c_3(2B^2 + r_1^2) \qquad r_1^2 = x_1^2 + y_1^2$$

Elimination of the x and y components in the above equations gives

$$[A_1^2 + k^2 - (\tfrac{3}{4}c_3B^2)^2]\, r_1^2 = 0 \tag{2.13}$$

from which the amplitude r_1 is found to be

$$r_1^2 = 0 \tag{2.14}$$

or $$r_1^2 = \left(\frac{4}{3} - 2B^2\right) \pm \sqrt{B^4 - \left(\frac{4k}{3c_3}\right)^2} \tag{2.15}$$

(ii) Second-harmonic Oscillation

Substituting Eq. (2.10) into (2.7) and equating the coefficients of the non-oscillatory term and of the terms containing $\sin 2\tau$ and $\cos 2\tau$ separately to zero, we obtain

$$\begin{aligned} -A_0z + \tfrac{3}{4}c_3B^2y_2 &\equiv Z(z, x_2, y_2) = 0 \\ -A_2x_2 - 2ky_2 &\equiv X_2(z, x_2, y_2) = 0 \\ 2kx_2 - A_2y_2 + \tfrac{3}{2}c_3B^2z &\equiv Y_2(z, x_2, y_2) = 0 \end{aligned} \tag{2.16}$$

where
$$\begin{aligned} A_0 &= -c_1-c_3[z^2+3/2(B^2+r_2^2)] \\ A_2 &= 4-c_1-3/4c_3(2B^2+4z^2+r_2^2) \\ r_2^2 &= x_2^2+y_2^2 \end{aligned}$$

Elimination of the x and y components in the above equations gives

$$\begin{aligned} -A_0z^2+1/2A_2r_2^2 &= 0 \\ (A_2^2+4k^2)r_2^2 &= (3/2c_3B^2)^2z^2 \end{aligned} \tag{2.17}$$

from which the unknown quantities z and r_2 are determined.

(iii) Third-harmonic Oscillation

Substituting Eq. (2.11) into (2.7) and equating the terms containing $\sin\tau$, $\cos\tau$, $\sin 3\tau$, and $\cos 3\tau$ separately to zero, we obtain

$$\begin{aligned} -(A_1+3/4c_3B^2)x_1-ky_1-3/4c_3[(x_1^2-y_1^2-B^2)x_3+2x_1y_1y_3] \\ \equiv X_1(x_1, y_1, x_3, y_3) = 0 \\ kx_1-(A_1-3/4c_3B^2)y_1+3/4c_3[2x_1y_1x_3-(x_1^2-y_1^2-B^2)y_3] \\ \equiv Y_1(x_1, y_1, x_3, y_3) = 0 \\ -A_3x_3-3ky_3+1/4c_3[3B^2-(x_1^2-3y_1^2)]x_1 \equiv X_3(x_1, y_1, x_3, y_3) = 0 \\ 3kx_3-A_3y_3+1/4c_3[3B^2-(3x_1^2-y_1^2)]y_1 \equiv Y_3(x_1, y_1, x_3, y_3) = 0 \end{aligned} \tag{2.18}$$

where
$$\begin{aligned} A_1 &= 1-c_1-3/4c_3(2B^2+r_1^2+2r_3^2) \\ A_3 &= 9-c_1-3/4c_3(2B^2+2r_1^2+r_3^2) \\ r_1^2 &= x_1^2+y_1^2 \qquad r_3^2 = x_3^2+y_3^2 \end{aligned}$$

from which the unknown quantities x_1, y_1, x_3, and y_3, and consequently the amplitudes, r_1 and r_3, are determined.

(*b*) *Stability Investigation of the Periodic Solutions*

The periodic solutions given above are sustained actually only when they are stable. In this section the stability of the periodic solutions will be investigated in the same manner as we have done in Sec. 1.3*b*. We consider a small variation $\xi(\tau)$ from the periodic solution $v_0(\tau)$. Then the behavior of $\xi(\tau)$ is described by the following variational equation

$$\frac{d^2\xi}{d\tau^2}+k\frac{d\xi}{d\tau}+\left(c_1+\frac{3}{2}c_3B^2+\frac{3}{2}c_3B^2\cos 2\tau+3c_3v_0^2\right)\xi = 0 \tag{2.19}$$

Furthermore we introduce a new variable $\eta(\tau)$ defined by

$$\xi(\tau) = e^{-\delta\tau}\cdot\eta(\tau) \qquad \delta = k/2 \tag{2.20}$$

to remove the first-derivative term. Then we obtain

$$\frac{d^2\eta}{d\tau^2}+\left(c_1-\delta^2+\frac{3}{2}c_3B^2+\frac{3}{2}c_3B^2\cos 2\tau+3c_3v_0^2\right)\eta = 0 \tag{2.21}$$

(i) Stability Condition for the Harmonic Oscillation

Inserting $v_0(\tau)$ as given by Eq. (2.9) into (2.21) leads to

$$\frac{d^2\eta}{d\tau^2}+(\theta_0+2\theta_{1s}\sin 2\tau+2\theta_{1c}\cos 2\tau)\eta = 0 \tag{2.22}$$

where
$$\theta_0 = c_1-\delta^2+\tfrac{3}{2}c_3(B^2+r_1^2)$$
$$\theta_{1s} = \tfrac{3}{2}c_3x_1y_1 \qquad \theta_{1c} = \tfrac{3}{4}c_3[B^2-(x_1^2-y_1^2)]$$

We assume that a particular solution of Eq. (2.22) in the first unstable region is given by

$$\eta(\tau) = e^{\mu\tau}\phi(\tau) = e^{\mu\tau}\sin(\tau-\sigma_1) \tag{2.23}$$

Proceeding analogously as in Sec. 1.3*b*, stability condition $|\mu|<\delta$ leads to

$$\Delta_1(\delta) \equiv \begin{vmatrix} \theta_0+\delta^2-1-\theta_{1c} & \theta_{1s}-2\delta \\ \theta_{1s}+2\delta & \theta_0+\delta^2-1+\theta_{1c} \end{vmatrix} \equiv \frac{\partial(X_1, Y_1)}{\partial(x_1, y_1)} > 0 \tag{2.24}$$

(ii) Stability Conditions for the Higher-harmonic Oscillations

The conditions for stability of the solutions given by Eqs. (2.10) and (2.11) may also be derived by the same procedure as above. The results are as follows.

Stability condition for solution (2.10):

$$\Delta_2(\delta) \equiv \frac{\partial(Z, X_2, Y_2)}{\partial(z, x_2, y_2)} > 0 \tag{2.25}$$

Stability condition for solution (2.11):

$$\Delta_3(\delta) \equiv \frac{\partial(X_1, Y_1, X_3, Y_3)}{\partial(x_1, y_1, x_3, y_3)} > 0 \tag{2.26}$$

The vertical tangency of the characteristic curves (Bz, Br_1, Br_2, and Br_3 relations) also occurs at the stability limit $\Delta_n(\delta)=0$ $(n=1, 2, 3)$.

NUMERICAL EXAMPLE

Putting $c_1=0$, and $c_3=1$ in Eq. (2.7) gives

$$\frac{d^2v}{d\tau^2}+k\frac{dv}{d\tau}+\frac{3}{2}B^2(1+\cos 2\tau)v+v^3 = 0$$

By use of Eqs. (2.15), (2.17), and (2.18) the amplitude characteristics of Eqs. (2.9), (2.10), and (2.11) were calculated for $k=0$ and 0.4. The result is plotted against B in Fig. 2.2. The dotted portions of the characteristic curves represent unstable states. It is to be mentioned that the portions of the B axis interposed between the end points of the characteristic curves are unstable. We see in the figure that increasing B will bring about the excitation of higher-harmonic oscillations and that once the oscillation is started, it may be stopped by decreasing B to a value which is lower than before, thus exhibiting the phenomenon of hysteresis.

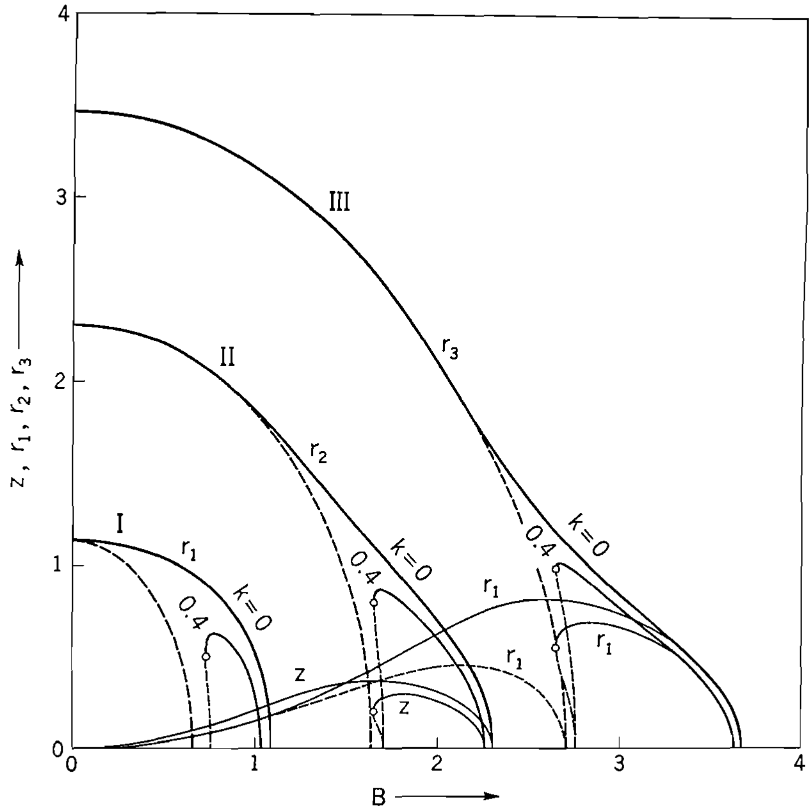

FIG. 2.2 Amplitude characteristics of the periodic solutions given by Eqs. (2.9), (2.10), and (2.11).

2.4 Solution of the Fundamental Equation Using Mapping Concepts

In this section we will give some examples of fixed points and correlated periodic solutions of Eq. (2.7) for the system parameters $k=0.4$, $c_1=0$, and $c_3=1$

$$\frac{d^2v}{d\tau^2}+0.4\frac{dv}{d\tau}+\frac{3}{2}B^2(1+\cos 2\tau)v+v^3=0 \tag{2.27}$$

The same method of analysis as in Sec. 1.5 is followed, and therefore only the stable solutions are discussed.

(*a*) *Numerical Analysis*

CASE 1. WHEN THE AMPLITUDE B OF THE EXTERNAL FORCE LIES IN THE FIRST UNSTABLE REGION

We consider the equation

$$\frac{d^2v}{d\tau^2}+0.4\frac{dv}{d\tau}+\frac{3}{2}(0.8)^2(1+\cos 2\tau)v+v^3=0 \tag{2.28}$$

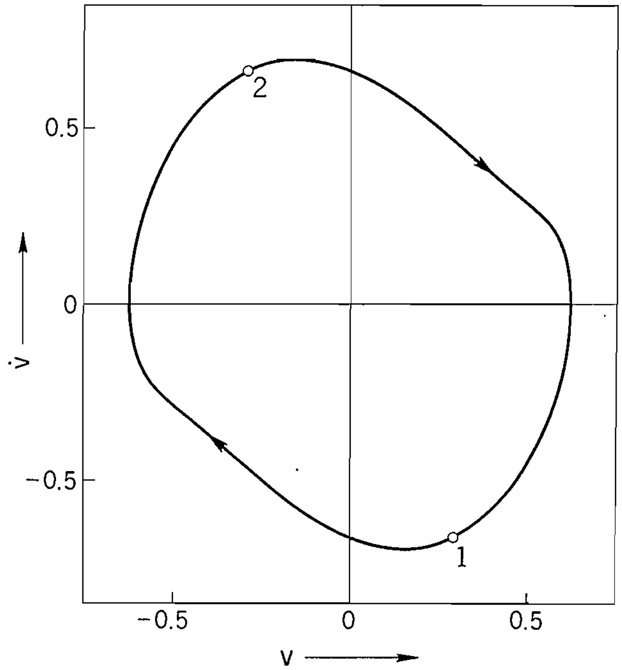

FIG. 2.3 Fixed points and trajectory of the stable solutions for Eq. (2.28).

For this particular value of B, there are two completely stable fixed points, 1 and 2. Each of them is obtained under every second iteration of the mapping.* Figure 2.3 shows the fixed points and the correlated trajectory. The periodic solutions, $v_{01}(\tau)$ and $v_{02}(\tau)$, corresponding to points 1 and 2, respectively, are given by

$$\begin{aligned} v_{01}(\tau) &= -v_{02}(\tau) \\ &= -0.55 \sin \tau + 0.29 \cos \tau - 0.04 \sin 3\tau + 0.00 \cos 3\tau \end{aligned} \tag{2.29}$$

CASE 2. WHEN THE AMPLITUDE B OF THE EXTERNAL FORCE LIES IN THE SECOND UNSTABLE REGION

As an example of such a case, we consider the equation

$$\frac{d^2v}{d\tau^2} + 0.4\frac{dv}{d\tau} + \frac{3}{2}(1.8)^2(1+\cos 2\tau)v + v^3 = 0 \tag{2.30}$$

There are two completely stable fixed points, 1 and 2. These fixed points and

* Equation (2.27) is written in the simultaneous form

$$\frac{dv}{d\tau} = \dot{v} \qquad \frac{d\dot{v}}{d\tau} = -0.4\dot{v} - \frac{3}{2}B^2(1+\cos 2\tau)v - v^3$$

where the right sides are periodic in τ with period π. Therefore the mapping T from $\tau = n\pi$ to $(n+1)\pi$ (n: integer) is considered.

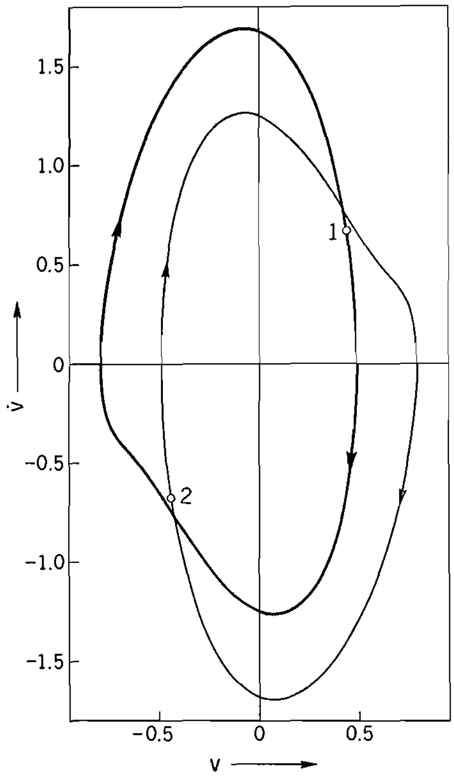

FIG. 2.4 Fixed points and trajectories of the stable solutions for Eq. (2.30).

the correlated trajectories are shown in Fig. 2.4. Corresponding to points 1 and 2 we have

$$\begin{aligned} v_{01}(\tau) &= -v_{02}(\tau) \\ &= -0.25+0.26 \sin 2\tau+0.55 \cos 2\tau+0.03 \sin 4\tau+0.13 \cos 4\tau \\ &\quad +0.00 \sin 6\tau+0.01 \cos 6\tau \end{aligned} \tag{2.31}$$

CASE 3. WHEN THE AMPLITUDE B OF THE EXTERNAL FORCE LIES IN THE THIRD UNSTABLE REGION

Putting $B=2.8$ in Eq. (2.27) gives

$$\frac{d^2v}{d\tau^2}+0.4\frac{dv}{d\tau}+\frac{3}{2}(2.8)^2(1+\cos 2\tau)v+v^3 = 0 \tag{2.32}$$

In this case there are two completely stable fixed points, 1 and 2, which are obtained under every second iteration of the mapping. Figure 2.5 shows the fixed points and the correlated trajectory. The corresponding periodic solutions are given by

$$\begin{aligned} v_{01}(\tau) &= -v_{02}(\tau) \\ &= \;\; 0.38 \sin \tau \; -0.06 \cos \tau \; -0.34 \sin 3\tau+0.16 \cos 3\tau \end{aligned}$$

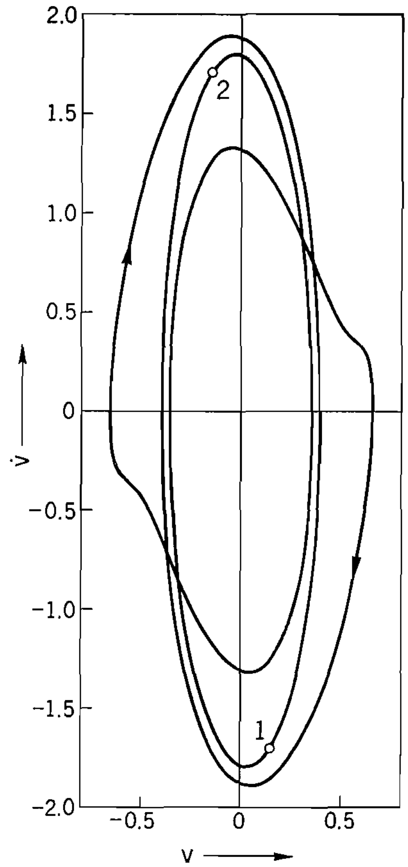

FIG. 2.5 Fixed points and trajectory of the stable solutions for Eq. (2.32).

$$-0.17 \sin 5\tau + 0.05 \cos 5\tau - 0.03 \sin 7\tau + 0.01 \cos 7\tau \qquad (2.33)$$

The details of the completely stable fixed points appearing in the above examples are summed up and listed in Table 2.1 with the related characteristic multipliers and the time increments h.

TABLE 2. 1 Completely Stable Fixed Points and Related Properties in Figs. 2. 3, 2. 4, and 2. 5

Fixed Point	B	v_0	$\dot{v}_0$	$\rho_{1,2}$	h
Fig. 2. 3 1	0.8	0.292	−0.662	$0.183 \pm 0.218i$	$\pi/30$
2	〃	−0.292	0.662	〃	〃
Fig. 2. 4 1	1.8	0.443	0.673	$0.430 \pm 0.316i$	$\pi/30$
2	〃	−0.443	−0.673	〃	〃
Fig. 2. 5 1	2.8	0.150	−1.704	$0.231 \pm 0.166i$	$\pi/60$
2	〃	−0.150	1.704	〃	〃

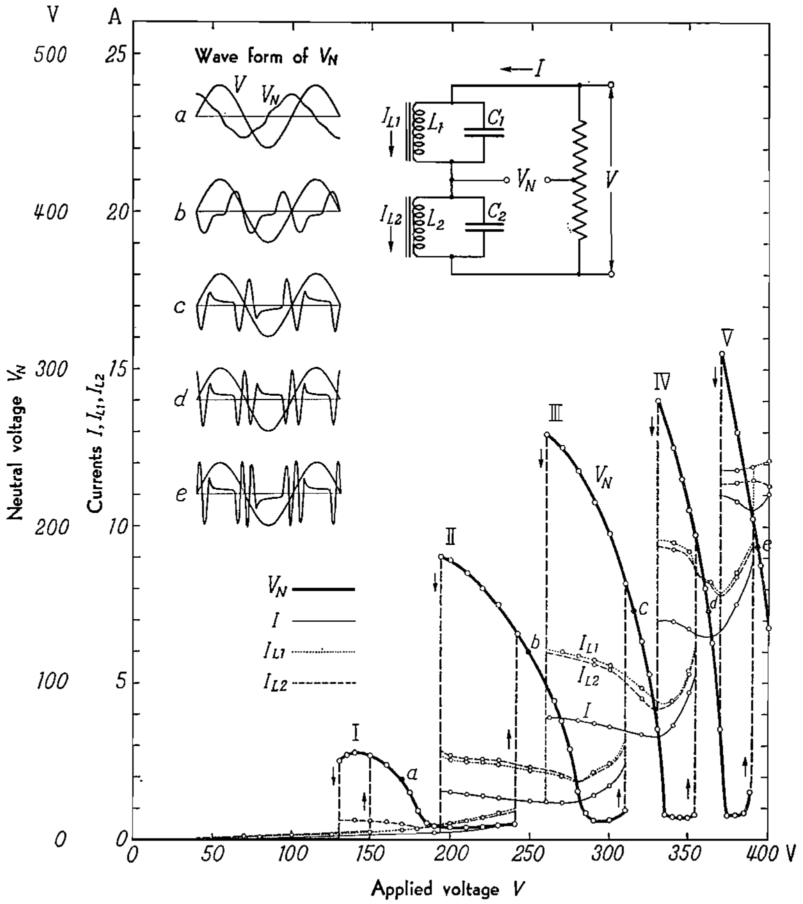

Fig. 2.6 Experimental result using parallel-resonance circuit.

2.5 Experimental Result

An experiment on the circuit of Fig. 2.1 has been performed [13, pp. 138–141]. The result is as follows.

The self-excitation of the fundamental and higher-harmonic oscillations was observed under varying E. As a result of the excitation of such a harmonic, the potential of the junction point of the two resonance circuits oscillates with respect to the neutral point of the applied voltage with the frequency of that harmonic. In Fig. 2.6, the anomalous neutral voltage V_N (which is related to the flux ϕ) is shown against the applied voltage.*

* The self-excited oscillation in the first unstable region (marked by I) has the same frequency as that of the applied voltage. See the waveform (a) in the figure. This phenomenon is known as the neutral inversion in electric transmission lines.

CHAPTER 3

ALMOST PERIODIC OSCILLATIONS IN A SELF-OSCILLATORY SYSTEM WITH EXTERNAL FORCE

3.1 Introduction

When a periodic force is applied to a nonlinear system, the resulting oscillation is usually, but not necessarily, periodic. When it is periodic, the fundamental period of the oscillation is the same as, or equal to an integral multiple of, the period of the external force. The terms harmonic and subharmonic oscillations are applied to these responses, respectively. There are also different cases in which the response of a nonlinear system is not periodic even when some transient has died out. Such a response will be referred to as an almost periodic oscillation. It is a salient feature of an almost periodic oscillation that the amplitude and the phase of the oscillation vary slowly, but periodically, even in the steady state. However, since the ratio between the period of the amplitude variation and that of the external force is in general incommensurable, there is no periodicity in this kind of oscillation.*

This chapter is concerned with the almost periodic oscillations which occur in a self-oscillatory system under periodic excitation. It is known that, when a periodic force is applied to a self-oscillatory system, the frequency of the self-excited oscillation, that is, the natural frequency of the system, falls in synchronism with the driving frequency, provided these two frequencies are not far different [2, 6, 9, 21, 29]. This phenomenon of frequency entrainment may also occur when the ratio of the two frequencies is in the neighborhood of an integer (different from unity) or a fraction [13, 22]. Thus, if the amplitude and the frequency of the external force are appropriately chosen, the natural frequency of the system is entrained by a frequency which is an integral multiple or a submultiple of the driving frequency. If the ratio of these two frequencies is not in the neighborhood of an integer or a fraction, we may expect the occurrence of an almost periodic oscillation [13, 28].

In this chapter, first, the regions of entrainment (such as, if the amplitude and the frequency of the external force are given in these regions, the entrainment occurs at the harmonic, higher-harmonic, or subharmonic frequency of the external force) will be studied by using the averaging method. Secondly, a limit cycle correlated with an almost periodic oscillation will be investigated. Finally, an almost periodic oscillation will be analyzed by applying the mapping procedure.

3.2 Van der Pol's Equation with Forcing Term

In the preceding chapters we treated the cases in which the restoring force of

* A detailed presentation of the theory of almost periodic functions can be found in Ref. 5.

the system was nonlinear. In this chapter we consider a system in which the nonlinearity appears in the damping. The system considered is governed by

$$\frac{d^2u}{dt^2}-\varepsilon(1-u^2)\frac{du}{dt}+u = B\cos\nu t+B_0 \tag{3.1}$$

where ε is a small positive constant and the right side represents an external force containing a nonoscillatory component. The left side of this equation takes the form of van der Pol's equation [25, 26]. Introduction of a new variable defined by $v=u-B_0$ yields an alternative form of Eq. (3.1)

$$\frac{d^2v}{dt^2}-\mu(1-\beta v-\gamma v^2)\frac{dv}{dt}+v = B\cos\nu t \tag{3.2}$$

where $\mu = (1-B_0^2)\varepsilon \qquad \beta = \dfrac{2B_0}{1-B_0^2} \qquad$ and $\qquad \gamma = \dfrac{1}{1-B_0^2}$

(a) *Forms of Entrained Oscillations*

Since μ is small, we see that when $B=0$ the natural frequency of the system (3.2) is nearly equal to unity. Hence, when the driving frequency ν is in the neighborhood of unity, we may expect an entrained oscillation at the driving frequency ν, that is, an occurrence of harmonic entrainment. The entrained harmonic oscillation $v_0(t)$ may be expressed approximately by

$$v_0(t) = b_1 \sin\nu t+b_2\cos\nu t \tag{3.3}$$

On the other hand, when the driving frequency ν is far different from unity, we may expect an occurrence of higher-harmonic or subharmonic entrainment. In this case, the entrained oscillation has a frequency which is an integral multiple or a submultiple of the driving frequency ν. An approximate solution for Eq. (3.2) may be expressed by

$$v_0(t) = \frac{B}{1-\nu^2}\cos\nu t+b_1\sin n\nu t+b_2\cos n\nu t \tag{3.4}$$

where $n = 2$ or 3: for higher-harmonic oscillations

$n = 1/2$ or $1/3$: for subharmonic oscillations

The first term in the right side represents the forced oscillation at the driving frequency ν. The second and the third terms represent the entrained oscillation at the frequency $n\nu$, which is close to unity.

(b) *Analog-computer Analysis*

In order to illustrate the phenomenon of frequency entrainment, we show some representative waveforms of various types of oscillations by making use of an analog computer. The system parameters under consideration are

$$\varepsilon = 0.2 \quad \text{and} \quad B_0 = 0.5$$

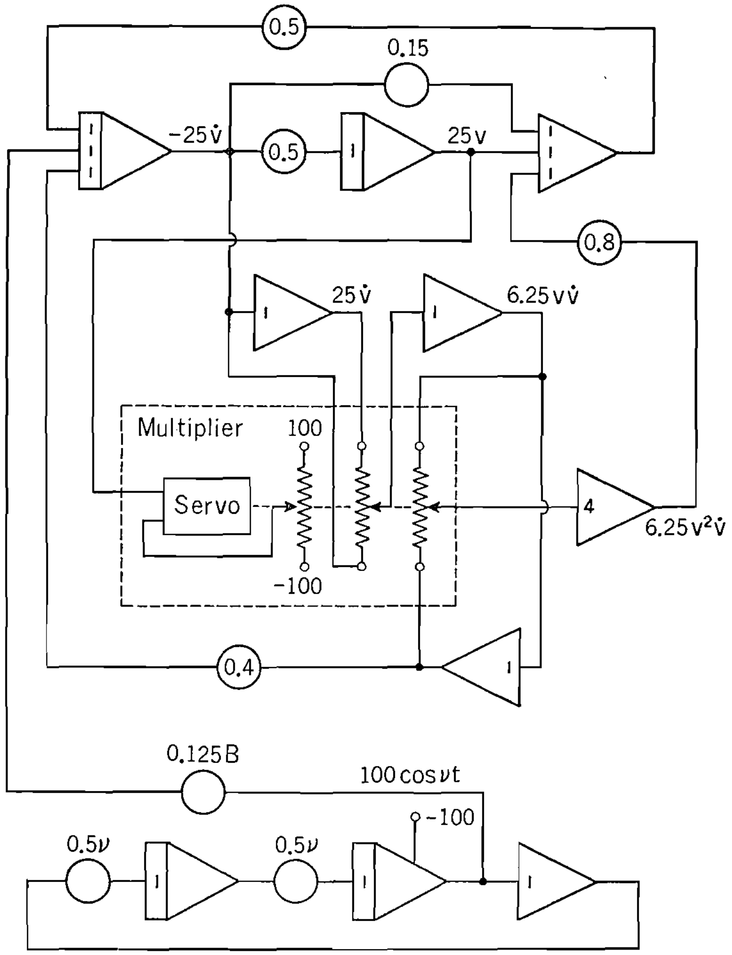

FIG. 3.1 Block diagram of an analog-computer setup for the solution of Eq. (3.5).

in Eq. (3.1). Consequently, the parameters in Eq. (3.2) are

$$\mu = 0.15 \quad \beta = 4/3 \quad \text{and} \quad \gamma = 4/3$$

then, Eq. (3.2) becomes

$$\frac{d^2v}{dt^2} - 0.15\left(1 - \frac{4}{3}v - \frac{4}{3}v^2\right)\frac{dv}{dt} + v = B\cos\nu t \tag{3.5}$$

Figure 3.1 shows the block diagram of an analog-computer setup for the solution of Eq. (3.5).* Some representative waveforms of $v(t)$ are shown in Fig. 3.2. The

* The integrating amplifiers in the block diagram integrate their inputs with respect to the machine time (in second), which is, in this particular case, 2 times the independent variable t.

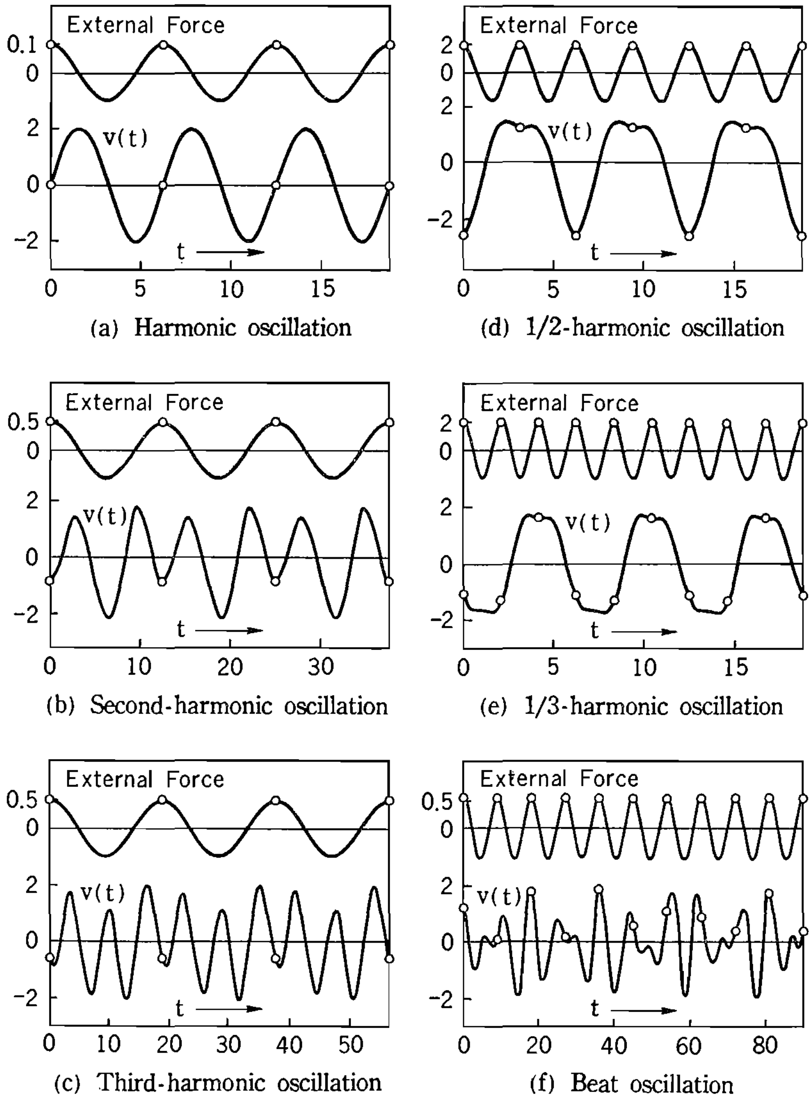

FIG. 3.2 Waveforms of the oscillations in the system described by Eq. (3.5) (obtained by analog-computer analysis).

TABLE 3.1 Amplitude and Frequency of the External Force in Fig. 3.2

Fig. 3.2	B	ν
a	0.1	1.00
b	0.5	0.50
c	0.5	0.33
d	2.0	1.99
e	2.0	2.97
f	0.55	0.70

points on the curves appear at the beginning of each cycle of the external force. The values of the amplitude B and the frequency ν of the external forces corresponding to Fig. 3.2 *a* to *f* are listed in Table 3.1.

3.3 Solution of van der Pol's Equation with Forcing Term Using Averaging Principle

(*a*) *Derivation of Autonomous Systems* [1, 4, 16]

We now write the differential equation (3.2) in a simultaneous form

$$\begin{aligned} \frac{dv}{dt} &= \dot{v} \\ \frac{d\dot{v}}{dt} &= \mu(1-\beta v-\gamma v^2)\dot{v}-v+B\cos\nu t \end{aligned} \tag{3.6}$$

The behavior of the system is described by the movement of a representative point $(v(t), \dot{v}(t))$ along the solution curves of Eqs. (3.6) in the $v\dot{v}$ plane. These solution curves are called trajectories of the representative point. Let us first consider the case in which the driving frequency ν of the external force is in the neighborhood of unity.* According to the form of the solution (3.3) considered in Sec. 3.2*a*, we introduce a new coordinate system $(b_1(t), b_2(t))$ defined by

$$\begin{aligned} v(t) &= b_1(t)\sin\nu t+ b_2(t)\cos\nu t \\ \dot{v}(t) &= \nu b_1(t)\cos\nu t-\nu b_2(t)\sin\nu t \end{aligned} \tag{3.7}$$

which rotates together with the representative point with angular frequency ν. It may therefore be conjectured that the coordinates $(b_1(t), b_2(t))$ of the representative point vary rather slowly in comparison with $(v(t), \dot{v}(t))$. To see this let us transform Eqs. (3.6) by using Eqs. (3.7). Hence

$$\begin{aligned} \frac{dx_1}{dt} = \frac{\mu}{2}\Big\{&\Big[(1-r_1^2)x_1-\sigma_1 y_1+\frac{B}{\mu\nu a_0}\Big]-\tfrac{1}{2}\beta a_0(x_1^2-y_1^2)\sin\nu t-\beta a_0 x_1 y_1\cos\nu t \\ &+[-\sigma_1 x_1-(1+2x_1^2-2y_1^2)y_1]\sin 2\nu t+\Big[(1-4y_1^2)x_1-\sigma_1 y_1+\frac{B}{\mu\nu a_0}\Big]\cos 2\nu t \\ &-\tfrac{1}{2}\beta a_0(x_1^2-y_1^2)\sin 3\nu t-\beta a_0 x_1 y_1\cos 3\nu t \\ &-(3x_1^2-y_1^2)y_1\sin 4\nu t+(x_1^2-3y_1^2)x_1\cos 4\nu t\Big\} \end{aligned}$$

$$\begin{aligned} \frac{dy_1}{dt} = \frac{\mu}{2}\Big\{&[\sigma_1 x_1+(1-r_1^2)y_1]-\beta a_0 x_1 y_1\sin\nu t+\tfrac{1}{2}\beta a_0(x_1^2-y_1^2)\cos\nu t \\ &+\Big[-(1-2x_1^2+2y_1^2)x_1+\sigma_1 y_1-\frac{B}{\mu\nu a_0}\Big]\sin 2\nu t+[-\sigma_1 x_1-(1-4x_1^2)y_1]\cos 2\nu t \end{aligned} \tag{3.8}$$

* It is here assumed that $\nu-1=O(\mu)$ and $B=O(\mu)$.

$$+\beta a_0 x_1 y_1 \sin 3\nu t - \tfrac{1}{2}\beta a_0 (x_1^2 - y_1^2)\cos 3\nu t$$
$$-(x_1^2 - 3y_1^2)x_1 \sin 4\nu t - (3x_1^2 - y_1^2)y_1 \cos 4\nu t\Big\}$$

where
$$x_1 = \frac{b_1}{a_0} \qquad y_1 = \frac{b_2}{a_0} \qquad r_1^2 = x_1^2 + y_1^2$$
$$a_0 = \sqrt{\frac{4}{\gamma}} \qquad \sigma_1 = \frac{1-\nu^2}{\mu\nu}\text{: detuning}$$

From the form of the right sides of Eqs. (3.8), it is seen that both dx_1/dt and dy_1/dt are proportional to the small parameter μ, so that x_1 and y_1 will be slowly varying functions of t as we have expected. Moreover dx_1/dt and dy_1/dt are periodic functions of t with period $2\pi/\nu$. It may therefore be considered that $x_1(t)$ and $y_1(t)$ remain approximately constant during one period $2\pi/\nu$. Hence averaging the right sides of Eqs. (3.8) over the period $2\pi/\nu$, we obtain the relations to determine dx_1/dt and dy_1/dt to a first approximation

$$\begin{aligned} \frac{dx_1}{dt} &= \frac{\mu}{2}\left[(1-r_1^2)x_1 - \sigma_1 y_1 + \frac{B}{\mu\nu a_0}\right] \equiv X_1(x_1, y_1) \\ \frac{dy_1}{dt} &= \frac{\mu}{2}\left[\sigma_1 x_1 + (1-r_1^2)y_1\right] \equiv Y_1(x_1, y_1) \end{aligned} \tag{3.9}$$

Equations (3.9) play an important role in the present investigation, since the singular points of this system correspond to the harmonic oscillations and the limit cycles, if exist, to the almost periodic oscillations. It is to be noted that x_1 and y_1 in Eqs. (3.9) denote the normalized amplitudes of the entrained oscillation since the constant a_0 represents the amplitude of the self-excited oscillation to a first approximation.

By the same procedure as above, we proceed next to derive the autonomous systems for the cases in which the frequency ν of the external force is in the neighborhood of an integer (different from unity) or a fraction.* In this case we make use of the transformation defined by

$$\begin{aligned} v(t) &= \frac{B}{1-\nu^2}\cos \nu t + b_1(t)\sin n\nu t + b_2(t)\cos n\nu t \\ \dot{v}(t) &= \frac{-\nu B}{1-\nu^2}\sin \nu t + n\nu b_1(t)\cos n\nu t - n\nu b_2(t)\sin n\nu t \end{aligned} \tag{3.10}$$

Then the derived autonomous systems are as follows.

$$n = 2: \quad \begin{aligned} \frac{dx_2}{dt} &= \frac{\mu}{2}\left[(D-r_2^2)x_2 - \sigma_2 y_2\right] \equiv X_2(x_2, y_2) \\ \frac{dy_2}{dt} &= \frac{\mu}{2}\left[\sigma_2 x_2 + (D-r_2^2)y_2 - \frac{\beta}{4a_0}A^2\right] \equiv Y_2(x_2, y_2) \end{aligned} \tag{3.11}$$

* It is also assumed that $\nu - 1/n = O(\mu)$ and $B = O(\mu)$.

$$n=3:\qquad \frac{dx_3}{dt}=\frac{\mu}{2}\Big[(D-r_3^2)x_3-\sigma_3 y_3\Big] \equiv X_3(x_3,\ y_3)$$
$$\frac{dy_3}{dt}=\frac{\mu}{2}\Big[\sigma_3 x_3+(D-r_3^2)y_3-\frac{r}{12a_0}A^3\Big] \equiv Y_3(x_3,\ y_3) \tag{3.12}$$

$$n=\tfrac{1}{2}:\ \frac{dx_{1/2}}{dt}=\frac{\mu}{2}\Big[\Big(D-r_{1/2}^2+\frac{1}{2}\beta A\Big)x_{1/2}-\sigma_{1/2}y_{1/2}\Big] \equiv X_{1/2}(x_{1/2},\ y_{1/2})$$
$$\frac{dy_{1/2}}{dt}=\frac{\mu}{2}\Big[\sigma_{1/2}x_{1/2}+\Big(D-r_{1/2}^2-\frac{1}{2}\beta A\Big)y_{1/2}\Big] \equiv Y_{1/2}(x_{1/2},\ y_{1/2}) \tag{3.13}$$

$$n=\tfrac{1}{3}:\ \frac{dx_{1/3}}{dt}=\frac{\mu}{2}\Big[(D-r_{1/3}^2)x_{1/3}-\sigma_{1/3}y_{1/3}+2\frac{A}{a_0}x_{1/3}y_{1/3}\Big] \equiv X_{1/3}(x_{1/3},\ y_{1/3})$$
$$\frac{dy_{1/3}}{dt}=\frac{\mu}{2}\Big[\sigma_{1/3}x_{1/3}+(D-r_{1/3}^2)y_{1/3}+\frac{A}{a_0}(x_{1/3}^2-y_{1/3}^2)\Big] \equiv Y_{1/3}(x_{1/3},\ y_{1/3}) \tag{3.14}$$

where
$$x_n=\frac{b_1}{a_0}\qquad y_n=\frac{b_2}{a_0}\qquad r_n^{\,2}=x_n^{\,2}+y_n^{\,2}$$
$$a_0=\sqrt{\frac{4}{r}}\qquad A=\frac{B}{1-\nu^2}\qquad D=1-\frac{2A^2}{a_0^2}$$
$$\sigma_n=\frac{1-(n\nu)^2}{\mu n\nu}:\ \text{detuning}$$

It is sometimes convenient to write Eqs. (3.13) and (3.14) using polar coordinates. By the transformation of coordinates $x_n=r_n\cos\theta_n$, $y_n=r_n\sin\theta_n$ with $n=\frac{1}{2}$ or $\frac{1}{3}$, Eqs. (3.13) and (3.14) are transferred as

$$\frac{dr_{1/2}}{dt}=\frac{\mu}{2}\Big[(D-r_{1/2}^2)r_{1/2}+\frac{\beta}{2}Ar_{1/2}\cos 2\theta_{1/2}\Big] \equiv R_{1/2}(r_{1/2},\ \theta_{1/2})$$
$$\frac{d\theta_{1/2}}{dt}=\frac{\mu}{2}\Big[\sigma_{1/2}-\frac{\beta}{2}A\sin 2\theta_{1/2}\Big] \equiv \Theta_{1/2}(\theta_{1/2}) \tag{3.13$_1$}$$

and
$$\frac{dr_{1/3}}{dt}=\frac{\mu}{2}\Big[(D-r_{1/3}^2)r_{1/3}+\frac{A}{a_0}r_{1/3}^2\sin 3\theta_{1/3}\Big] \equiv R_{1/3}(r_{1/3},\ \theta_{1/3})$$
$$\frac{d\theta_{1/3}}{dt}=\frac{\mu}{2}\Big[\sigma_{1/3}+\frac{A}{a_0}r_{1/3}\cos 3\theta_{1/3}\Big] \equiv \Theta_{1/3}(r_{1/3},\ \theta_{1/3}) \tag{3.14$_1$}$$

It is to be noted that Eqs. (3.13$_1$) are unchanged if $\theta_{1/2}$ is replaced by $\theta_{1/2}+\pi$, while Eqs. (3.14$_1$) are unchanged if $\theta_{1/3}$ is replaced by $\theta_{1/3}+2\pi/3$. This implies that the singular points and the integral curves of (3.13$_1$) are π symmetric with respect to the origin and those of (3.14$_1$) are $2\pi/3$ symmetric.

(*b*) *Singular Points Correlated with Periodic Oscillations*

Let x_{10} and y_{10} be the coordinates of the singular point of Eqs. (3.9). They are obtained by putting $dx_1/dt=0$ and $dy_1/dt=0$

$$X_1(x_{10}, y_{10}) = 0 \qquad Y_1(x_{10}, y_{10}) = 0 \tag{3.15}$$

and represent the particular solution corresponding to the equilibrium state of this system. The variational equations for this solution are of the form

$$\frac{d\xi}{dt} = a_1\xi + a_2\eta \qquad \frac{d\eta}{dt} = b_1\xi + b_2\eta \tag{3.16}$$

with $a_1 = \left(\frac{\partial X_1}{\partial x_1}\right)_0$, $a_2 = \left(\frac{\partial X_1}{\partial y_1}\right)_0$, $b_1 = \left(\frac{\partial Y_1}{\partial x_1}\right)_0$, and $b_2 = \left(\frac{\partial Y_1}{\partial y_1}\right)_0$

where $\left(\frac{\partial X_1}{\partial x_1}\right)_0, \cdots, \left(\frac{\partial Y_1}{\partial y_1}\right)_0$ denote the values of $\frac{\partial X_1}{\partial x_1}, \cdots, \frac{\partial Y_1}{\partial y_1}$ at $x_1 = x_{10}$ and $y_1 = y_{10}$, respectively, and are constants.

Let us assume that the characteristic equation of this system has no root the real part of which is equal to zero. It is known that in this case the system (3.8) has for sufficiently small μ one and only one periodic solution which reduces to the solution $x_1 = x_{10}$ and $y_1 = y_{10}$ for $\mu = 0$. Moreover the stability of this solution is decided by the sign of the real parts of the corresponding characteristic roots. That is, if the real parts of the roots of the characteristic equation of the system (3.16) are negative, the corresponding periodic solution is stable; if at least one root has a positive real part, the periodic solution is unstable [4].

The coordinates of the singular point are given by

$$x_{10} = -\frac{\mu\nu a_0}{B}(1 - r_{10}^2) r_{10}^2 \qquad y_{10} = \frac{\mu\nu a_0}{B}\sigma_1 r_{10}^2 \tag{3.17}$$

where r_{10}^2 is determined by the equation

$$\left[(1 - r_{10}^2)^2 + \sigma_1^2\right] r_{10}^2 = \left(\frac{B}{\mu\nu a_0}\right)^2 \tag{3.18}$$

Equation (3.18) yields what we call the amplitude characteristics (response curves) for the harmonic oscillation and is obtained by eliminating x_{10} and y_{10} from Eqs. (3.15). Figure 3.3 is obtained by plotting Eq. (3.18) in the $r_{10}^2\sigma_1$ plane for various values of the magnitude $(B/\mu\nu a_0)^2$. Evidently the curves are symmetrical with respect to the r_{10}^2 axis. Each point on these curves yields the amplitude r_{10}, which is correlated with the frequency ν of a possible harmonic oscillation for a given value of the amplitude B.

Proceeding in the same manner as above the coordinates of the singular points for the derived autonomous systems (3.11), (3.12), (3.13), and (3.14) and the relations representing the amplitude characteristic of the entrained oscillations are easily known. They are enumerated as follows.*

* In order to avoid the troublesome notation we hereafter omit the subscript 0 which designates the state of equilibrium.

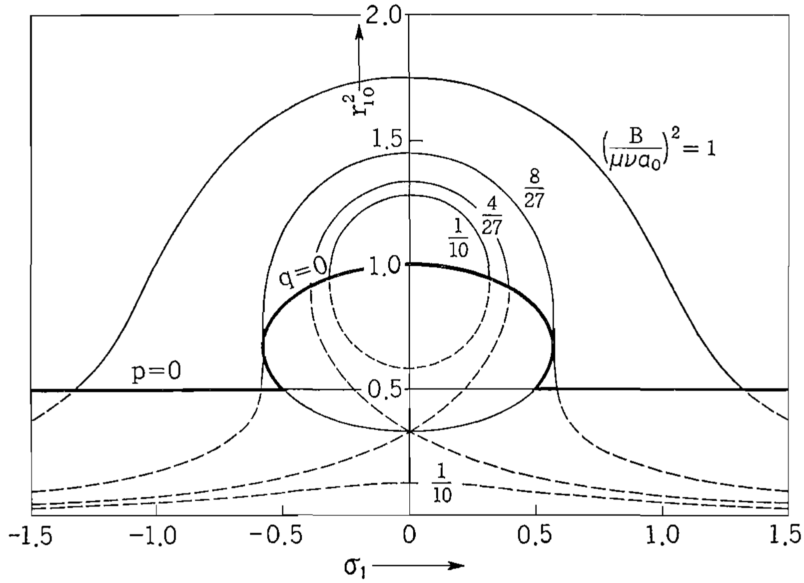

FIG. 3.3 Normalized response curves for the harmonic oscillation.

For the system (3.11):

$$x_2 = \frac{4a_0\sigma_2}{\beta A^2} r_2^2 \qquad y_2 = \frac{4a_0(D-r_2^2)}{\beta A^2} r_2^2 \tag{3.19}$$

$$\left[(D-r_2^2)^2+\sigma_2^2\right] r_2^2 = \left(\frac{\beta}{4a_0} A^2\right)^2 \tag{3.20}$$

For the system (3.12):

$$x_3 = \frac{12a_0\sigma_3}{\gamma A^3} r_3^2 \qquad y_3 = \frac{12a_0(D-r_3^2)}{\gamma A^3} r_3^2 \tag{3.21}$$

$$\left[(D-r_3^2)^2+\sigma_3^2\right] r_3^2 = \left(\frac{\gamma}{12a_0} A^3\right)^2 \tag{3.22}$$

For the system (3.13):

$$\begin{aligned} x_{1/2} &= r_{1/2}\cos\theta_{1/2} \qquad r_{1/2}\cos(\theta_{1/2}+\pi) \\ y_{1/2} &= r_{1/2}\sin\theta_{1/2} \qquad r_{1/2}\sin(\theta_{1/2}+\pi) \end{aligned} \tag{3.23}$$

where $\cos 2\theta_{1/2} = \dfrac{-2(D-r_{1/2}^2)}{\beta A} \qquad \sin 2\theta_{1/2} = \dfrac{2\sigma_{1/2}}{\beta A}$

$$\left[(D-r_{1/2}^2)^2+\sigma_{1/2}^2-\frac{1}{4}\beta^2A^2\right] r_{1/2}^2 = 0 \tag{3.24}$$

For the system (3.14):

$$\begin{aligned} x_{1/3} &= r_{1/3}\cos\theta_{1/3} \quad r_{1/3}\cos\left(\theta_{1/3}+\frac{2\pi}{3}\right) \quad r_{1/3}\cos\left(\theta_{1/3}+\frac{4\pi}{3}\right) \\ y_{1/3} &= r_{1/3}\sin\theta_{1/3} \quad r_{1/3}\sin\left(\theta_{1/3}+\frac{2\pi}{3}\right) \quad r_{1/3}\sin\left(\theta_{1/3}+\frac{4\pi}{3}\right) \end{aligned} \tag{3.25}$$

where $\cos 3\theta_{1/3} = \dfrac{-a_0\sigma_{1/3}}{Ar_{1/3}} \qquad \sin 3\theta_{1/3} = \dfrac{-a_0(D-r_{1/3}^2)}{Ar_{1/3}}$

$$\left[(D-r_{1/3}^2)^2+\sigma_{1/3}^2-\frac{r}{4}A^2r_{1/3}^2\right]r_{1/3}^2 = 0 \tag{3.26}$$

We will notice from Eqs. (3.24) and (3.26) that the origin of the $x_n y_n$ plane ($n=$ 1/2 or 1/3) is always a singular point.

(*c*) *Conditions for Stability of Singular Points*

The periodic states of equilibrium of the initial system (3.2) are not always realized, but are actually able to exist only so long as they are stable. We have already seen that the stability of the harmonic solution of Eq. (3.2) is to be decided in accordance with the characteristic roots of the corresponding singular point (3.17). In this section we will therefore consider the stability condition for the singular point.

Let ξ and η be small variations from the singular point defined by

$$x_1 = x_{10}+\xi \qquad y_1 = y_{10}+\eta \tag{3.27}$$

and determine whether these variations approach zero or not with the increase of time t. We again write the variational equations (3.16) which are obtained by substituting Eqs. (3.27) into (3.9) and neglecting terms of higher degree than the first in ξ and η

$$\frac{d\xi}{dt} = a_1\xi+a_2\eta \qquad \frac{d\eta}{dt} = b_1\xi+b_2\eta \tag{3.28}$$

where
$$\begin{aligned} a_1 &= \frac{\mu}{2}(1-r_{10}^2-2x_{10}^2) \qquad & a_2 &= \frac{\mu}{2}(-\sigma_1-2x_{10}y_{10}) \\ b_1 &= \frac{\mu}{2}(\sigma_1-2x_{10}y_{10}) \qquad & b_2 &= \frac{\mu}{2}(1-r_{10}^2-2y_{10}^2) \end{aligned}$$

The characteristic equation of the system (3.28) is given by

$$\begin{vmatrix} a_1-\lambda & a_2 \\ b_1 & b_2-\lambda \end{vmatrix} = 0$$

or
$$\lambda^2+p\lambda+q = 0 \tag{3.29}$$

where
$$\begin{aligned} p &= -(a_1+b_2) = \mu(2r_{10}^2-1) \\ q &= a_1b_2-a_2b_1 = \frac{\mu^2}{4}\left[(1-r_{10}^2)(1-3r_{10}^2)+\sigma_1^2\right] \end{aligned}$$

The variations ξ and η approach zero with the time t, provided that the real part of λ is negative. This stability condition is given by the Routh-Hurwitz criterion [15], that is

$$p > 0 \quad \text{and} \quad q > 0 \tag{3.30}$$

On Fig. 3.3 the stability limits $p = 0$ and $q = 0$ are also drawn; the curve $p=0$ is a horizontal line $r_{10}^2=1/2$, and the curve $q = 0$ is an ellipse which is the locus of the vertical tangents of the response curves. The unstable portions of the response curves are shown dotted in the figure. We can obtain the region of harmonic entrainment on the $B\nu$ plane by reproducing the stability limit (drawn by thick line in the figure) of Fig. 3.3. The portions of the ellipse $q = 0$ applies in the case where the amplitude B and consequently the detuning σ_1 are comparatively small, while if B and σ_1 are large the stability limit $p = 0$ applies. For the intermediate values of B and σ_1 some complicated phenomena may occur, but we will not enter this problem here. A detailed investigation about such cases is reported by Cartwright [6] and Stoker [29].

We discuss, for the time being, a classification of singular points of Eqs. (3.9). Poincaré [24] classified the types of singular points according to the character of the integral curves near the singular points, that is, according to the nature of the characteristic roots λ. They are as follows.

1. The singularity is a nodal point (or simply a node) if the characteristic roots are both real and of the same sign, so that

$$p^2-4q \geqq 0 \quad \text{and} \quad q > 0 \tag{3.31}$$

2. The singularity is a saddle point if the two roots are real but of opposite sign, so that

$$q < 0 \tag{3.32}$$

3. The singularity is a focal point (or a focus) if the two roots are complex conjugates, so that

$$p^2-4q < 0 \tag{3.33}$$

If, in particular, both the roots are purely imaginary so that $p = 0$, the singularity is either a center or a focus.*

Proceeding in the same manner as above, we obtain the stability conditions for

* Following the above classification, the type of singularity will be definite when the characteristic roots λ_1 and λ_2 are neither zero nor purely imaginary. Such a singularity is called simple or of the first kind. However there still remain special cases in which the characteristic equation has a zero root or a purely imaginary root. In this case, the corresponding singular points are said to be of the higher order or of the second kind. Such singularity appears corresponding to a point on the stability limits $p=0$ and $q=0$ of Fig. 3.3 except the portion of $p=0$ within the ellipse $q=0$. In such a situation, the existence of a periodic solution of the initial system (3.2) is not in general guaranteed or the stability of the periodic solution is not decided by the above criterion even if the existence is certified. The details of such bifurcation problem are reported by Yorinaga [31].

the singular points of the autonomous systems (3.11) to (3.14). They are as follows.
For the system (3.11):

$$p_2 = \mu(2r_2^2 - D) > 0 \qquad q_2 = \frac{\mu^2}{4}\left[(D - r_2^2)(D - 3r_2^2) + \sigma_2^2\right] > 0 \tag{3.34}$$

For the system (3.12):

$$p_3 = \mu(2r_3^2 - D) > 0 \qquad q_3 = \frac{\mu^2}{4}\left[(D - r_3^2)(D - 3r_3^2) + \sigma_3^2\right] > 0 \tag{3.35}$$

For the system (3.13):

$$p_{1/2} = -\mu D > 0 \quad q_{1/2} = \frac{\mu^2}{4}\left(D^2 - \frac{1}{4}\beta^2 A^2 + \sigma_{1/2}^2\right) > 0 \quad (\text{for } r_{1/2} = 0) \tag{3.36$_1$}$$

$$p_{1/2} = \mu(2r_{1/2}^2 - D) > 0 \quad q_{1/2} = \mu^2 r_{1/2}^2 (r_{1/2}^2 - D) > 0 \quad (\text{for } r_{1/2} \neq 0) \tag{3.36$_2$}$$

For the system (3.14):

$$p_{1/3} = -\mu D > 0 \quad q_{1/3} = \frac{\mu^2}{4}\left(D^2 + \sigma_{1/3}^2\right) > 0 \quad (\text{for } r_{1/3} = 0) \tag{3.37$_1$}$$

$$p_{1/3} = \mu(2r_{1/3}^2 - D) > 0 \quad q_{1/3} = -\frac{3}{2}\mu^2 r_{1/3}^2\left(D + \frac{\gamma}{8}A^2 - r_{1/3}^2\right) > 0 \quad (\text{for } r_{1/3} \neq 0) \tag{3.37$_2$}$$

NUMERICAL EXAMPLE (REGIONS OF FREQUENCY ENTRAINMENT)

Thus far, the singular points of the derived autonomous systems (3.9), (3.11), (3.12), (3.13), and (3.14) and the relations representing the amplitude characteristic of the entrained oscillations have been investigated. The stability for these singular points has also been investigated by making use of the Routh-Hurwitz criterion. From these results we can obtain the regions of frequency entrainment on the $B\nu$ plane; namely, if the amplitude B and the frequency ν of the external force are given in these regions, the corresponding autonomous system possesses at least one stable singularity. Consequently, entrainment occurs at the corresponding harmonic, higher-harmonic, or subharmonic frequency of the external force. Figure 3.4 shows an example of the regions of frequency entrainment for the same parameters as in Sec. 3.2*b*, that is

$$\varepsilon = 0.2 \quad \text{and} \quad B_0 = 0.5$$

so that

$$\mu = 0.15 \quad \beta = 4/3 \quad \text{and} \quad \gamma = 4/3$$

We see that the higher-harmonic or subharmonic entrainment occurs within a narrow range of the driving frequency ν. On the other hand, the harmonic entrainment occurs at any driving frequency ν provided the amplitude B of the external force is sufficiently large.

In Fig. 3.4*a* the boundary curves of the higher-harmonic entrainment tend asymptotically to the curve $D = 0$ as the detuning $\sigma_n (n = 2, 3)$ increases. In the figure the curve $D = 0$ is plotted by dashed line. We see that the inequality

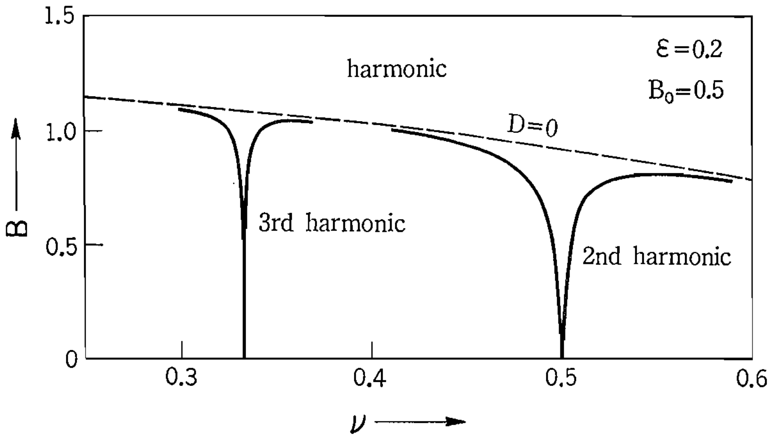

(a) Harmonic and higher-harmonic entrainments.

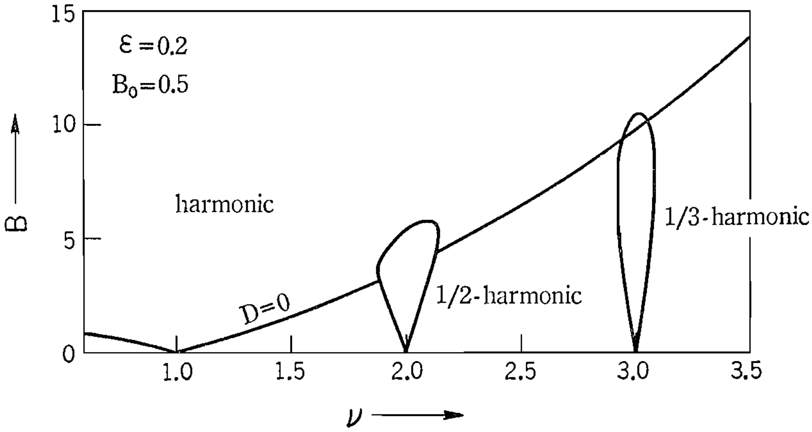

(b) Harmonic and subharmonic entrainments.

FIG. 3.4 Regions of frequency entrainment.

$$D = 1 - \frac{2A^2}{a_0^2} < 0 \tag{3.38}$$

is equivalent to the first condition of (3.30) which gives the boundary of harmonic entrainment for large detuning σ_1.* The stability conditions (3.34) and (3.35)

* Since μ is small, the condition $\sigma_1^2 \gg (1-r_{10}^2)^2$ is satisfied when ν is not in the neighborhood of unity. Under this condition, we obtain from Eq. (3.18) the following approximation

$$a_0^2 r_{10}^2 \cong \left(\frac{B}{1-\nu^2}\right)^2 = A^2$$

With the above result the first condition of (3.30) is replaced by the inequality (3.38). However it is to be noted that the assumptions made in the derivation of Eqs. (3.9) becomes inappropriate as the detuning σ_1 increases.

show that, if $D<0$ the higher-harmonic oscillations are stable. Furthermore since there are no abrupt changes in the amplitudes of the higher-harmonic components of an oscillation at the curve $D=0$, the boundary curve $D=0$ of the harmonic entrainment has practically no significance.

In Fig. 3.4*b*, the boundary of harmonic entrainment in the neighborhood of $\nu=1$ ($\sigma_1=0$) is given by the second condition of (3.30) for small detuning σ_1 and by the first condition for large detuning σ_1.* For larger values of the detuning σ_1 this boundary curves are approximated by the curve $D=0$ as we have seen before and this boundary continues to the curve given by the first conditions of (3.36_1) and (3.37_1) which are the stability conditions for the harmonic component only, since $r_n=0$ ($n=1/2$, $1/3$) means no subharmonic component.

It is also mentioned that the regions of harmonic and 1/3-harmonic entrainments have an overlapping area. In this area common to the two regions, both the harmonic and the 1/3-harmonic oscillations are sustained. On the other hand, such a situation does not occur for the 1/2-harmonic entrainment.

The results of Fig. 3.4 are also compared with the regions obtained by using an analog computer. The block diagram of Fig. 3.1 is used. It is confirmed that the regions thus obtained agree well with that of Fig. 3.4.

(*d*) *Limit Cycles Correlated with Almost Periodic Oscillations*

The oscillations governed by van der Pol's equation with forcing term are characterized by the behavior of the representative point of the derived autonomous systems within the accuracy of the approximation made in the averaging principle. Now suppose that we fix a point ($x_n(0)$, $y_n(0)$) in the x_ny_n plane as an initial condition. Then the representative point moves, with the increase of time t, along the integral curve which emanates from the initial point and leads ultimately into a stable singular point. Thus the transient solutions are correlated with the integral curves, and the stationary periodic solutions, with the singular points in the x_ny_n plane. However the representative point may not always lead to a singular point, but may tend to a closed trajectory along which it moves permanently. An isolated trajectory such that no trajectory sufficiently near it is also closed is called a limit cycle.** In such a case we see that $x_n(t)$ and $y_n(t)$ tend to periodic functions having the same period in t and hence the solution of the original differential equation (3.2) will be one in which the amplitude and the phase after the lapse of sufficient time vary slowly but periodically. In the same way that a singular point represents a periodic solution of the initial system, a limit cycle represents a stationary oscillation which is affected by amplitude and phase modulation.

* As we noticed that, for the intermediate values of σ_1, the boundary becomes complicated, but we overlooked these situations in Fig. 3.4*b*, since such ranges of the external force are extremely limited.

** Occurrences of such a special solution were first studied by Poincaré [24]. See also Refs. 8, and 21.

The closed trajectory C is said to be orbitally stable if, given $\varepsilon > 0$, there is $\eta > 0$ such that, if R is a representative point of another trajectory which is within a distance η from C at time t_0, then R remains within a distance ε from C for $t > t_0$. If no such η exists, C is orbitally unstable. Moreover if C is orbitally stable and, in addition, if the distance between R and C tends to zero as t increases, C is said to be asymptotically orbitally stable.

The stability (orbital) of a limit cycle can be tested by making use of the Poincaré's criterion for orbital stability. This stability criterion is the following inequality [29]

$$\oint_C \left(\frac{\partial X_n}{\partial x_n} + \frac{\partial Y_n}{\partial y_n}\right) dt < 0 \tag{3.39}$$

We proceed to establish the existence of a limit cycle when the external force is given outside the regions of frequency entrainment. In such a case it follows from a careful consideration that there is only one singular point in the $x_n y_n$ plane. Furthermore, this singular point is identified as an unstable focus. This means that any representative point starting near this singularity moves away from it with increasing t; in fact there is an ellipse containing the focus in its interior with the property that all representative points cross it on moving from its interior to its exterior as t increases. On the other hand, all integral curves of the autonomous systems remain, as t increases, within a circle of sufficiently large radius. This

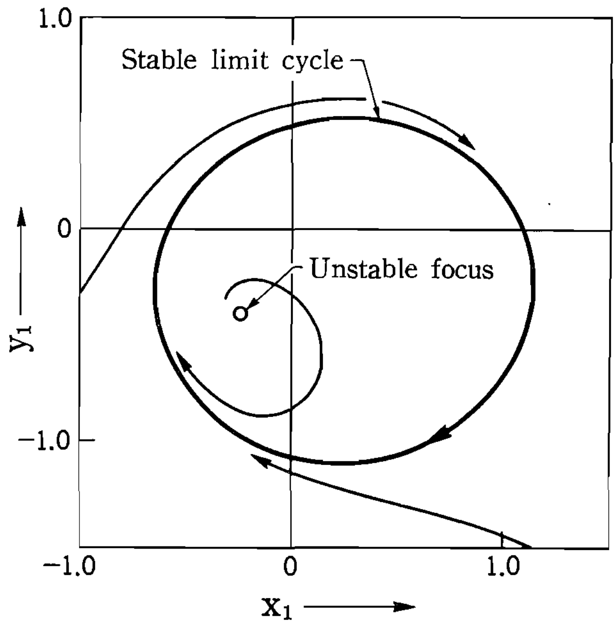

FIG. 3.5 Integral curves and limit cycle of Eqs. (3.9) in the case when B=0.2 and ν=1.1.

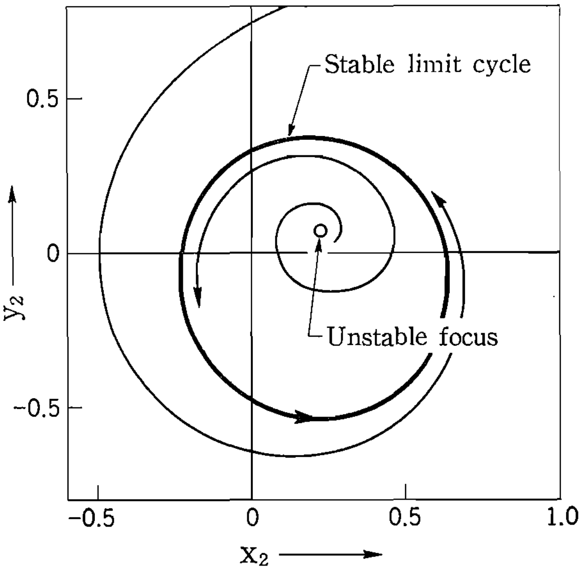

FIG. 3.6*a* Integral curves and limit cycle of Eqs. (3.11) in the case when $B=0.8$ and $\nu=0.47$.

follows at once from the form of the autonomous systems, since we have approximately for large x_n and y_n: $\frac{dx_n}{dt}=-\frac{\mu}{2}r_n^2x_n$ and $\frac{dy_n}{dt}=-\frac{\mu}{2}r_n^2y_n$, so that $\frac{dy_n}{dx_n}=\frac{y_n}{x_n}$. This means that the integral curves are approximately the rays through the origin and that a representative point on one of them moves toward the origin as t increases. Thus there is a ring-shaped domain bounded on the outside by this circle and on the inside by a small ellipse which is free from singular points and has the property that any solution curve which starts inside it remains there as t increases. The theorem of Poincaré and Bendixson [8, 21] can therefore be applied to establish the existence of at least one limit cycle.

Thus far, the existence of a limit cycle for the derived autonomous systems is proved. However, it is in general not easy to obtain any further information (number, location, shape, or size) about the limit cycle. In order to determine the limit cycle precisely, we are compelled to resort to numerical or graphical means.

NUMERICAL EXAMPLE (LIMIT CYCLES)

We will give some examples of the limit cycle when the amplitude B and the frequency ν of the external force are prescribed closed to the regions of entrainment.* The system parameters considered are the same as those in Secs. 3.2*b* and

* When B and ν of the external force are given just between but not near the regions of entrainment, the assumptions made in the derivation of the autonomous systems become inappropriate. Consequently, the almost periodic oscillation in such case may well be approximated by a sum of two simple harmonic components, one with the natural frequency of the system and the other with the driving frequency [29].

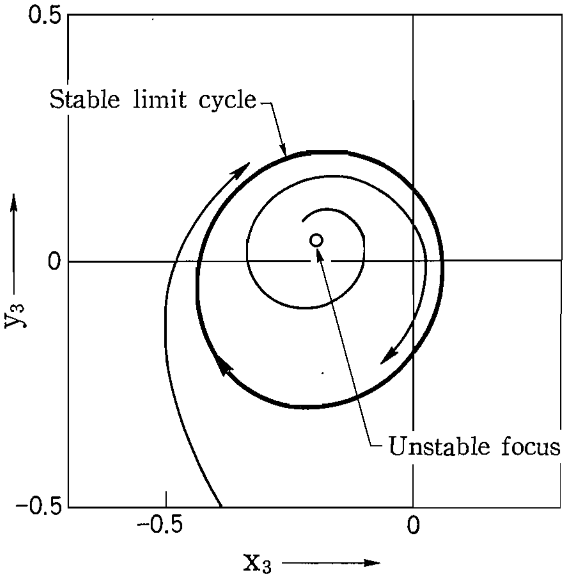

FIG. 3.6*b* Integral curves and limit cycle of Eqs. (3.12) in the case when $B=1.0$ and $\nu=0.345$.

3.3*c*, that is

$$\varepsilon = 0.2 \quad \text{and} \quad B_0 = 0.5$$

so that

$$\mu = 0.15 \quad \beta = 4/3 \quad \text{and} \quad \gamma = 4/3$$

CASE 1. WHEN THE EXTERNAL FORCE IS PRESCRIBED JUST OUTSIDE THE REGION OF HARMONIC ENTRAINMENT, i.e.,

$$B = 0.2 \quad \text{AND} \quad \nu = 1.1$$

In this case the autonomous system (3.9) is used. The limit cycle is pursued both from the outside and from the inside by carrying out the numerical integration of Eqs. (3.9) and is shown in Fig. 3.5.* Thus it is identified that the limit cycle is asymptotically orbitally stable. The period required for the representative point $(x_1(t), y_1(t))$ to complete one revolution along the limit cycle is 13.07···times the period $2\pi/\nu$ of the external force.**

CASE 2. WHEN THE EXTERNAL FORCES ARE PRESCRIBED JUST OUTSIDE THE REGIONS OF HIGHER-HARMONIC ENTRAINMENT, i.e.,

(*a*) $B = 0.8$ AND $\nu = 0.47$

(*b*) $B = 1.0$ AND $\nu = 0.345$

* The numerical integration using the Runge-Kutta-Gill's process was carried out on the KDC-I Digital Computer.

** Refer to Appendix for further details of the limit cycle of Fig. 3. 5.

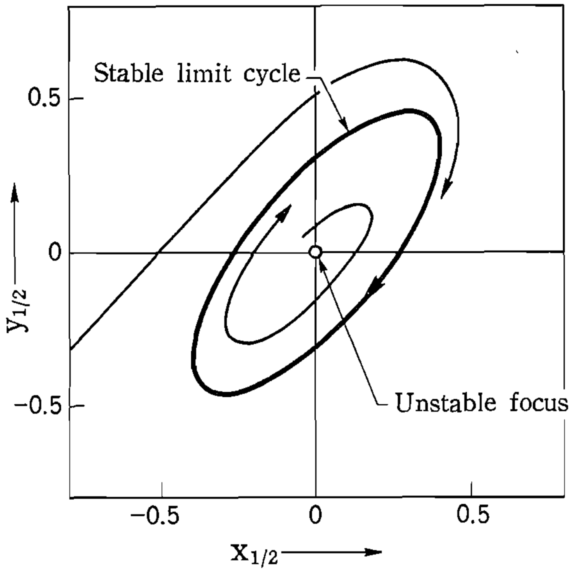

FIG. 3.7*a* Integral curves and limit cycle of Eqs. (3.13) in the case when B=4.0 and ν=2.15.

In Figs. 3.6*a* and *b* are plotted the limit cycles of Eqs. (3.11) and (3.12) for the above parameters, respectively. They are determined in much the same way as above. The periods required for the representative points to complete one revolution along the limit cycles of Figs. 3.6*a* and *b* are 7.81··· and 10.29··· times the period of the external force, respectively.

CASE 3. WHEN THE EXTERNAL FORCES ARE PRESCRIBED JUST OUTSIDE THE REGIONS OF SUBHARMONIC ENTRAINMENT, i.e.,

(*a*) $B = 4.0$ AND $\nu = 2.15$

(*b*) $B = 6.7$ AND $\nu = 2.85$

By making use of Eqs. (3.13) and (3.14) the limit cycles of such cases are determined and are shown in Figs. 3.7*a* and *b*. The periods required for the representative points to complete one revolution along the limit cycles of Figs. 3.7*a* and *b* are 45.93··· and 68.32··· times the period of the external force, respectively.

TABLE 3. 2 Unstable Foci and Related Properties in Figs. 3. 5, 3. 6, and 3. 7

Singular Point	B	ν	x_n	y_n	$\lambda_{1,2}$
Fig. 3. 5	0.2	1.1	−0.245	−0.400	$0.042 \pm 0.094i$
Fig. 3.6*a*	0.8	0.47	0.226	0.066	$0.014 \pm 0.062i$
Fig. 3.6*b*	1.0	0.345	−0.195	0.043	$0.005 \pm 0.034i$
Fig. 3.7*a*	4.0	2.15	0	0	$0.014 \pm 0.047i$
Fig. 3.7*b*	6.7	2.85	0	0	$0.031 \pm 0.051i$

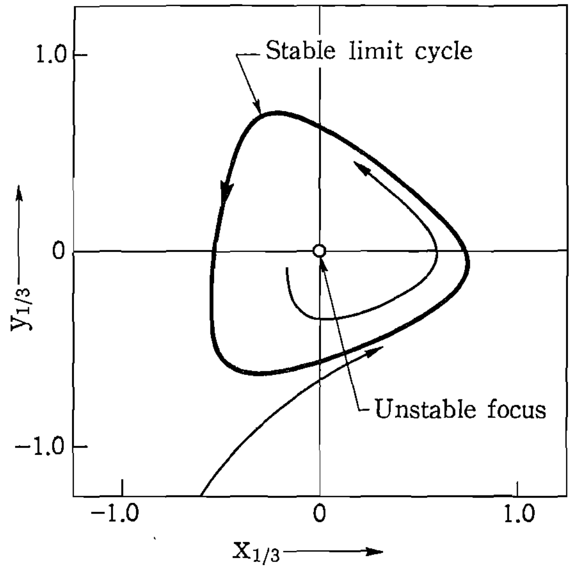

FIG. 3.7*b* Integral curves and limit cycle of Eqs. (3.14) in the case when B=6.7 and ν=2.85.

The details of the unstable foci appearing in the above examples are summed up and listed in Table 3.2. There are also given the characteristic roots of the corresponding variational equations.

3.4 Analysis of Almost Periodic Oscillations Using Mapping Concepts

We again write Eq. (3.2) in the simultaneous form

$$\begin{aligned}\frac{dv}{dt} &= \dot{v}\\ \frac{d\dot{v}}{dt} &= \mu(1-\beta v-\gamma v^2)\dot{v}-v+B\cos\nu t\end{aligned} \tag{3.40}$$

We see that the right sides are analytic in v, $\dot{v}$, and t, and are periodic in t with period $2\pi/\nu$.

In much the same way as described in Sec. 1.5, Eqs. (3.40) define the topological mapping T of the $v\dot{v}$ plane into itself. In this section, for almost periodic oscillations, the behavior of the image points under the mapping T will be investigated.

(*a*) *Invariant Closed Curves under the Mapping*

We have seen in the preceding sections that when the amplitude B and the frequency ν of the external force are given outside the regions of entrainment, the corresponding autonomous system possesses at least one stable limit cycle. In such a situation it has been tacitly assumed that to the periodic solution of the autonomous system represented by the limit cycle there actually corresponds an almost periodic solution of the initial system. Such assertion will, however, in general requires examination. But when the limit cycle is strongly stable, it is known that there exists a unique correspondence between the limit cycle of the autonomous system (3.9) and the simple closed curve which is invariant under the mapping defined by Eqs. (3.8) and differs little from the limit cycle provided μ is sufficiently small.* The closed curve invariant under the mapping is called an invariant closed curve.

The invariant closed curve C is said to be a completely stable invariant closed curve under T if (*a*) it divides the plane into two open simply connected invariant continua, S_i and S_e where to S_e is adjoined the point at infinity; (*b*) every point of C is a limit point of S_i or of S_e or of both; and (*c*) for any small ε there exists an open continuum, $0(\varepsilon)$ containing C, with a distance from C less than ε and such that

$$\lim_{n\to\infty} T^n(0(\varepsilon)) = C$$

A curve is said to be a completely unstable invariant closed curve if it is a completely stable invariant closed curve under the inverse mapping, i.e., T^{-1}. This definition is due to Levinson [17].

Let us denote an invariant closed curve under the mapping T by C and consider the solutions of Eqs. (3.40) with initial values on C when $t=0$, or the mapping of C into itself. For $0\leqq t\leqq 2\pi/\nu$, these solutions form a surface in $v\dot{v}t$ space which is bounded by C when $t=0$ and $t=2\pi/\nu$. Thus we see that this surface is a homeomorph of a closed torus. The problem of the solutions of Eqs. (3.40) which emanate from C is reduced to the problem of the solution of a differential equation on a torus. This type of differential equations has been investigated in detail and we will give an outline of the character of this type of equations in what follows.

(*b*) *Differential Equations on a Torus and Rotation Numbers* [8, 10]

In general a differential equation on a torus can be written in the form

$$\frac{dx}{dt} = p(t, x) \tag{3.41}$$

where it is assumed that

(i) $p(t, x)$ and $\partial p(t, x)/\partial x$ are real continuous functions defined for all real t, and x, and

(ii) $p(t+1, x) = p(t, x+1) = p(t, x)$

Because of (i) and (ii), $p(t, x)$ is bounded and hence every solution of Eq. (3.41) exists for all t. The periodicity assumption (ii) implies that $p(t, x)$ may be considered as a function on the surface of a torus R, the points of which can be described by Cartesian coordinates (t, x), where two points $P_1(t_1, x_1)$ and $P_2(t_2, x_2)$ are regarded as identical if t_1-t_2 and x_1-x_2 are integers. Similarly let $x=\varphi(t)$ be a solution of

* For the definition of strong stability and the justification of this statement, see Cartwright [7]. See also Bogoliuboff and Mitropolsky [4].

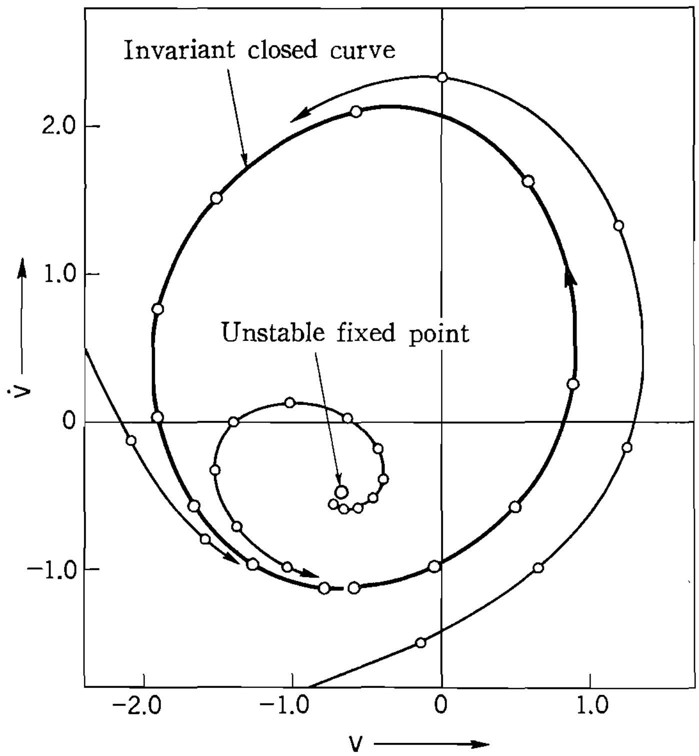

FIG. 3.8 Loci of image points and invariant closed curve for Eq. (3.48).

Eq. (3.41), the solution curve $(t, \varphi(t))$ may be represented on R.

Let $x=\varphi(t, \eta)$ be the solution of Eq. (3.41) such that $\varphi(0, \eta)=\eta$. From the assumption (ii) and the relation $\varphi(0, \eta)+1=\eta+1$, we obtain

$$\varphi(t, \eta+1) = \varphi(t, \eta)+1 \tag{3.42}$$

Consider the function $\psi(\eta)$ defined by

$$\psi(\eta) = \varphi(1, \eta) \tag{3.43}$$

From the assumption (i) it follows that $\psi(\eta)$ is a continuous function of η. From Eqs. (3.42) and (3.43), we obtain

$$\psi(\eta+1) = \psi(\eta)+1 \tag{3.44}$$

It follows from the uniqueness of solutions that no two solution curves may cross each other on R, and hence $\psi(\eta)$ must be a continuous monotone increasing function for all real η. Let C be the circle on R defined at $t=0$, then the function $\psi(\eta)$ induces a topological mapping M of C into C and we denote this by

$$P_1 = MP_0 \tag{3.45}$$

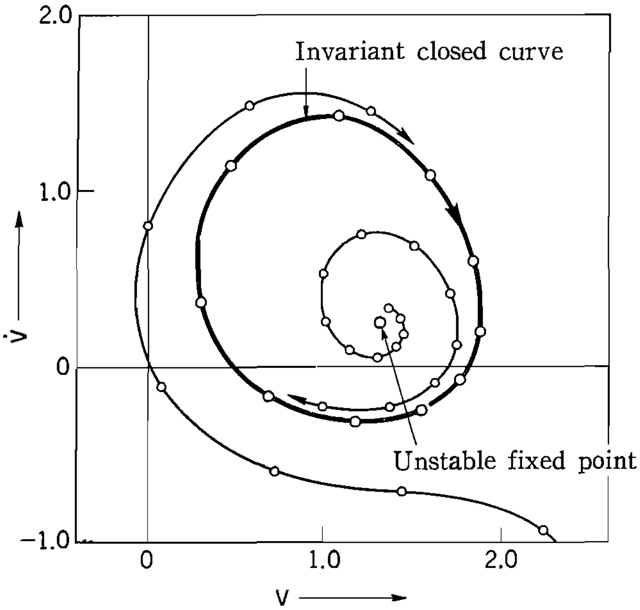

FIG. 3.9*a* Loci of image points and invariant closed curve for Eq. (3.49).

where $P_0=(0, \eta)$, $P_1=(1, \varphi(1, \eta))=(0, \psi(\eta))$. Thus the investigation of the nature of the solution curves of Eq. (3.41) on R can now be carried out by studying the topological mapping M and its representing real function $\psi(\eta)$.

Let ψ^2 be the function defined by $\psi^2(\eta)=\psi(\psi(\eta))$, and, in general, $\psi^n(\eta)=\psi(\psi^{n-1}(\eta))$ for any integer n, where it is understood that $\psi^0(\eta)=\eta$. Then we define a number ρ by the limit

$$\rho = \lim_{|n|\to\infty} \frac{\psi^n(\eta)}{n} \tag{3.46}$$

This number ρ is called the rotation number of M for Eq. (3.41). It is known that this limit exists and is independent of the solution used to define it, or the choice of η. This number ρ measures the average advance of a solution φ of Eq. (3.41) starting at $(0, \eta)$ as t changes by a unit.

The nature of the solution curves of Eq. (3.41) on R or of the mapping M is characterized by this number.

If ρ is rational and of the form p/q where p and q have no common factors, then Eq. (3.41) has periodic solutions on R of period q in t. Any non-periodic solution must tend toward such a periodic solution as t increases indefinitely. In this situation Eq. (3.41) has among its solutions subharmonics of order q.

If ρ is irrational there are two possibilities. One of these possibilities is termed the singular case. In case the right side of Eq. (3.41) satisfies some hypothesis, for instance, besides the assumptions (i) and (ii), $\partial^2 p/\partial x^2$ exists and is con-

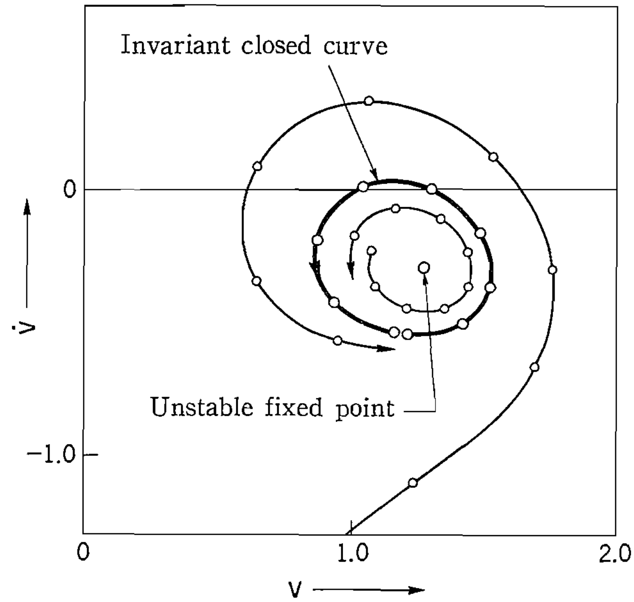

FIG. 3.9*b* Loci of image points and invariant closed curve for Eq. (3.50).

tinuous, the singular case cannot occur. Under this circumstance (termed the ergodic case) the solutions of Eq. (3.41) can be written in the form

$$\varphi(t) = \rho t + c + \omega(t, \rho t + c) \tag{3.47}$$

where ρ is the rotation number, c is an arbitrary constant, and $\omega(u, v)$ is a function continuous and periodic in u and v of period 1. Equation (3.41) has almost periodic solutions on R of t in this case.

(*c*) *Numerical Analysis*

We will here show some numerical examples of invariant closed curves of Eqs. (3.40) and calculate the rotation numbers correlated with them. The successive images $P_n(v(2n\pi/\nu), \dot{v}(2n\pi/\nu))$ $(n=1, 2, 3, \cdots)$ of the initial point $P_0(v(0), \dot{v}(0))$ under the mapping T are obtained by using the KDC-I Digital Computer. In performing the numerical integration, we used the Runge-Kutta-Gill's method. The same system parameters are used as those in the preceding examples. The values of B and ν of the external force are also same as those in Sec. 3.3*d*.

CASE 1. WHEN THE EXTERNAL FORCE IS PRESCRIBED JUST OUTSIDE THE REGION OF HARMONIC ENTRAINMENT

We consider the case corresponding to Fig. 3.5 in which $B=0.2$ and $\nu=1.1$ and the equation becomes

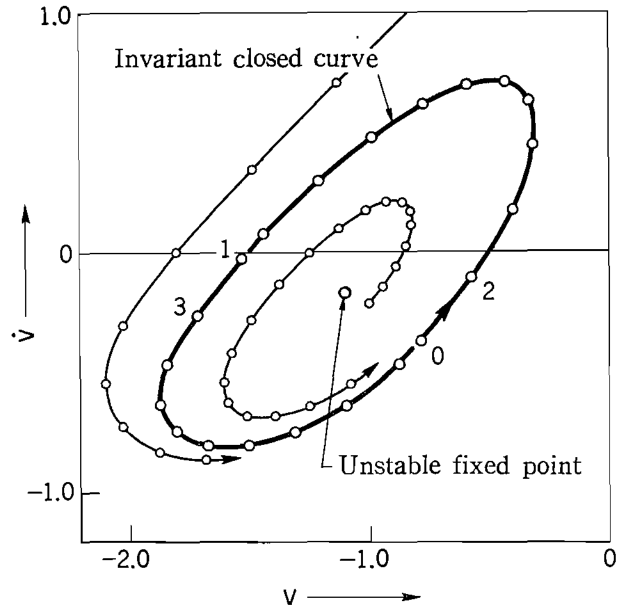

FIG. 3.10*a* Loci of image points and invariant closed curve for Eq. (3.51).

$$\frac{d^2v}{dt^2}-0.15\left(1-\frac{4}{3}v-\frac{4}{3}v^2\right)\frac{dv}{dt}+v=0.2\cos 1.1t \tag{3.48}$$

The unstable fixed point and the invariant closed curve of Eq. (3.48) are shown in Fig. 3.8. The small circles on the curves represent examples of the image points under the mapping T, and they are transferred successively to the points that follow in the direction of the arrows. In the figure some invariant curves which tend toward invariant closed curve on both sides are also shown. Thus we see that this invariant closed curve is completely stable.

CASE 2. WHEN THE EXTERNAL FORCES ARE PRESCRIBED JUST OUTSIDE THE REGIONS OF HIGHER-HARMONIC ENTRAINMENT

Corresponding to Figs. 3.6*a* and *b*, we consider the following two equations.

(a)
$$\frac{d^2v}{dt^2}-0.15\left(1-\frac{4}{3}v-\frac{4}{3}v^2\right)\frac{dv}{dt}+v=0.8\cos 0.47t \tag{3.49}$$

(b)
$$\frac{d^2v}{dt^2}-0.15\left(1-\frac{4}{3}v-\frac{4}{3}v^2\right)\frac{dv}{dt}+v=1.0\cos 0.345t \tag{3.50}$$

The unstable fixed points and the invariant closed curves of Eqs. (3.49) and (3.50) are shown in Figs. 3.9*a* and *b*, respectively. We see in the figures that these invariant closed curves are also completely stable.

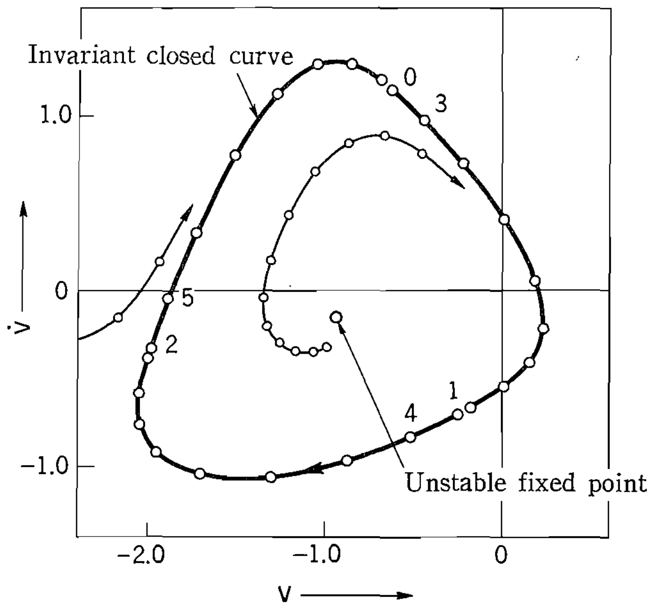

FIG. 3.10*b* Loci of image points and invariant closed curve for Eq. (3.52).

CASE 3. WHEN THE EXTERNAL FORCES ARE PRESCRIBED JUST OUTSIDE THE REGIONS OF SUBHARMONIC ENTRAINMENT

We consider the cases corresponding to Figs. 3.7*a* and *b*, and the equations become

(a) $$\frac{d^2v}{dt^2}-0.15\left(1-\frac{4}{3}v-\frac{4}{3}v^2\right)\frac{dv}{dt}+v = 4.0\cos 2.15t \qquad (3.51)$$

(b) $$\frac{d^2v}{dt^2}-0.15\left(1-\frac{4}{3}v-\frac{4}{3}v^2\right)\frac{dv}{dt}+v = 6.7\cos 2.85t \qquad (3.52)$$

In the systems described by the above equations, we have situations considerably different from those of the other examples. The unstable fixed points and the completely stable invariant closed curves are shown in Figs. 3.10*a* and *b*, respectively. The numbers in the figures designate the order of appearance of the image points. In Fig. 3.10*a* the neighboring image points on the curves are transferred in the direction of the arrows under every second iteration of the mapping, while in Fig. 3.10*b* under every third iteration of the mapping. On account of this property, it is natural that the invariant curves and the rotation numbers should be considered under T^2 or T^3 in stead of under T, when the external forces are given near the regions of subharmonic entrainment.

The rotation numbers correlated with the invariant closed curves of Figs. 3.8, 3.9, and 3.10 are listed in Table 3.3. There are also given the coordinates of the unstable fixed points (obtained by making use of the inverse mapping in much the same way as in Sec. 1.5*c*) and the time increments h which are employed for carrying out the numerical integration.

TABLE 3. 3 Rotation Numbers Correlated with Invariant Closed Curves and Unstable Fixed Points in Figs. 3. 8, 3. 9, and 3. 10

	ρ	v_0	$\dot{v}_0$	h
Fig. 3.8	0.0879···	−0.673	−0.478	$\pi/12\nu$
Fig. 3.9*a*	0.100···	1.322	0.246	$\pi/24\nu$
Fig. 3.9*b*	0.121···	1.271	−0.292	$\pi/24\nu$
Fig. 3.10*a*	0.0502···*	−1.099	−0.167	$\pi/12\nu$
Fig. 3.10*b*	0.0417···*	−0.938	−0.145	$\pi/12\nu$

* Rotation Numbers under T^2 and T^3 are listed.

APPENDIX

STABILITY OF PERIODIC SOLUTIONS OF AUTONOMOUS SYSTEMS

In this appendix we will study the problem of stability of periodic solutions of autonomous systems. We consider the second order autonomous system governed by

$$\frac{dx}{dt} = X(x, y) \qquad \frac{dy}{dt} = Y(x, y) \tag{1}$$

where the right sides are nonlinear functions of x and y, and we here assume that they are analytic with respect to those variables. Let $x=\varphi(t)$, $y=\psi(t)$ be its periodic solution with period τ and let $\xi(t)$, $\eta(t)$ be small variations defined by

$$x(t) = \varphi(t)+\xi(t) \qquad y(t) = \psi(t)+\eta(t) \tag{2}$$

Then the variational system has the form

$$\frac{d\xi}{dt} = p_{11}(t)\,\xi+p_{12}(t)\,\eta \qquad \frac{d\eta}{dt} = p_{21}(t)\,\xi+p_{22}(t)\,\eta \tag{3}$$

where

$$p_{11}(t) = \left(\frac{\partial X}{\partial x}\right)_{\substack{x=\varphi(t)\\ y=\psi(t)}} \qquad p_{12}(t) = \left(\frac{\partial X}{\partial y}\right)_{\substack{x=\varphi(t)\\ y=\psi(t)}}$$

$$p_{21}(t) = \left(\frac{\partial Y}{\partial x}\right)_{\substack{x=\varphi(t)\\ y=\psi(t)}} \qquad p_{22}(t) = \left(\frac{\partial Y}{\partial y}\right)_{\substack{x=\varphi(t)\\ y=\psi(t)}}$$

Equations (3) are linear differential equations with periodic coefficients. Since the system (1) is autonomous and its periodic solution $(\varphi(t), \psi(t))$ is not a state of equilibrium, it is known that the variational system (3) necessarily has one characteristic multiplier equal to unity. We denote the other by ρ, then

$$\rho = \exp\left[\int_0^\tau (p_{11}(t)+p_{22}(t))\,dt\right] \tag{4}$$

Thus if

$$\int_0^\tau (p_{11}(t)+p_{22}(t))\,dt < 0$$

then the periodic solution $(\varphi(t), \psi(t))$ is Lyapunov stable.* The periodic solution $(\varphi(t), \psi(t))$ is called a rough limit cycle when $\rho \neq 1$. It is stable for $\rho < 1$ and unstable for $\rho > 1$.

Numerical Example

Let us consider the autonomous system (3.9), that is,

* For the definition of Lyapunov stability and the details of this statement, see Pontryagin [27].

$$\begin{aligned}\frac{dx_1}{dt} &= \frac{\mu}{2}\left[(1-r_1^2)x_1-\sigma_1 y_1+\frac{B}{\mu\nu a_0}\right] \equiv X_1(x_1, y_1)\\ \frac{dy_1}{dt} &= \frac{\mu}{2}\left[\sigma_1 x_1+(1-r_1^2)y_1\right] \qquad \equiv Y_1(x_1, y_1)\end{aligned} \tag{5}$$

A periodic solution represented by the limit cycle of Fig. 3.5 (in which $\mu=0.15$, $\beta=\gamma=4/3$, $B=0.2$, and $\nu=1.1$) is given by

$$\begin{aligned} x_1(t) = \varphi_1(t) &= 0.09+0.19\sin\theta \ -0.81\cos\theta\\ &\quad -0.19\sin 2\theta+0.06\cos 2\theta\\ &\quad +0.04\sin 3\theta+0.04\cos 3\theta+\cdots\\ y_1(t) = \psi_1(t) &= -0.42+0.74\sin\theta \ +0.17\cos\theta\\ &\quad -0.06\sin 2\theta-0.17\cos 2\theta\\ &\quad -0.03\sin 3\theta+0.04\cos 3\theta+\cdots\\ \theta &= 0.0841\cdots\times(t-h)\end{aligned} \tag{6}$$

where h is an arbitrary constant. The period τ of this solution is approximately $74.68(=2\pi/\nu\times 13.07\cdots)$. The variational equations corresponding to the solution (6) are

$$\frac{d\xi}{dt} = p_{11}(t)\xi+p_{12}(t)\eta \qquad \frac{d\eta}{dt} = p_{21}(t)\xi+p_{22}(t)\eta \tag{7}$$

where $p_{11}(t) = \frac{\mu}{2}(1-3\varphi_1^2(t)-\psi_1^2(t))$ $\qquad p_{12}(t) = \frac{\mu}{2}(-\sigma_1-2\varphi_1(t)\psi_1(t))$

$p_{21}(t) = \frac{\mu}{2}(\sigma_1-2\varphi_1(t)\psi_1(t))$ $\qquad p_{22}(t) = \frac{\mu}{2}(1-\varphi_1^2(t)-3\psi_1^2(t))$

One of the characteristic multiplier ρ is given by

$$\begin{aligned}\rho &= \exp\left[\mu\int_0^\tau (1-2\varphi_1^2(t)-2\psi_1^2(t))\,dt\right]\\ &= \exp\left[\mu\tau(1-2\bar{r}_1^2)\right] = \exp(-8.20) = 0.000275\end{aligned} \tag{8}$$

where $\qquad \bar{r}_1^2 = \frac{1}{\tau}\int_0^\tau (\varphi_1^2(t)+\psi_1^2(t))\,dt = 0.866$

The magnitude $\bar{r}_1$ is sometimes called a normalized r.m.s. (root mean square) amplitude of an almost periodic oscillation.

REFERENCES

1. Andronov, A. A., A. A. Vitt, and S. E. Khaikin: "Theory of Oscillators," Fizmatgiz, Moscow, 1963 (in Russian); English translation, Pergamon Press, London, 1966.
2. Andronow, A. A., and A. A. Witt: Zur Theorie des Mitnehmens von van der Pol, *Arch. Elektrotech.*, **24**: 99–110 (1930).
3. Blair, K. W., and W. S. Loud: Periodic Solutions of $x''+cx'+g(x)=Ef(t)$ under Variation of Certain Parameters, *J. Soc. Ind. Appl. Math.*, **8**: 74–101 (1960).
4. Bogoliuboff, N. N., and Yu. A. Mitropolsky: "Asymptotic Methods in the Theory of Nonlinear Oscillations, " Fizmatgiz, Moscow, 1963 (in Russian); English translation, Gordon and Breach, Science Publishers, Inc., New York, 1961.
5. Bohr, H.: Zur Theorie der fastperiodischen Funktionen, *Acta Math.*, **45**: 29–127 (1924); **46**: 101–214 (1925); **47**: 237–281 (1926).
6. Cartwright, M. L.: Forced Oscillations in Nearly Sinusoidal Systems, *J. Inst. Elec. Engrs. (London)*, **95**: 88–96 (1948).
7. Cartwright, M. L.: Forced Oscillations in Nonlinear Systems, 149–241 in "Contributions to the Theory of Nonlinear Oscillations," **1** (1950), *Ann. Math. Studies*, no. 20, Princeton University Press, Princeton, N.J.
8. Coddington, E. A., and N. Levinson: "Theory of Ordinary Differential Equations," McGraw-Hill Book Company, New York, 1955.
9. Cunningham, W. J.: "Introduction to Nonlinear Analysis," McGraw-Hill Book Company, New York, 1958.
10. Denjoy, A.: Sur les courbes définies par les équations différentielles à la surface du tore, *J. Math.*, **9-11**: 333–375 (1932).
11. Duffing, G.: "Erzwungene Schwingungen bei veränderlicher Eigenfrequenz und ihre technische Bedeutung," Sammlung Vieweg, Braunschweig, 1918.
12. Floquet, G.: Sur les équations différentielles linéaires à coefficients périodiques, *Ann. Ecole Norm. Super.*, **2-12**: 47–88 (1883).
13. Hayashi, C.: "Nonlinear Oscillations in Physical Systems," McGraw-Hill Book Company, New York, 1964.
14. Hill, G. W.: On the Part of the Motion of the Lunar Perigee, *Acta Math.*, **8**: 1–36 (1886).
15. Hurwitz, A.: Über die Bedingungen, unter Welchen eine Gleichung nur Wurzeln mit negativen reellen Teilen besitzt, *Math. Ann.*, **46**: 273–284 (1895).
16. Kryloff, N., and N. Bogoliuboff: "Introduction to Nonlinear Mechanics," translated from the Russian by S. Lefschetz, *Ann. Math. Studies*, no. 11, Princeton, N.J., 1947.
17. Levinson, N.: Transformation Theory of Non-linear Differential Equations of the Second Order, *Ann. Math.*, **45**: 723–737 (1944). Correction **49**: 738 (1948).
18. McLachlan, N. W.: "Theory and Application of Mathieu Functions," Oxford University Press, London, 1947.
19. Malkin, I. G.: "Some Problems in the Theory of Nonlinear Oscillations," Gostekhizdat, Moscow, 1956 (in Russian); English translation, OTS Atomic Energy Commission, Washington, D.C.
20. Mathieu, É.: Mémoire sur le mouvement vibratoire d'une membrance de forme elliptique, *J. Math.*, **2-13**: 137–203 (1868).
21. Minorsky, N.: "Nonlinear Oscillations," D. Van Nostrand Company, Inc., Princeton, N. J., 1962.

22. Nag, B. R.: Ultraharmonic and Subharmonic Resonance in an Oscillator, *J. Brit. IRE,* **19:** 411–416 (1959).
23. Nishikawa, Y.: "A Contribution to the Theory of Nonlinear Oscillations," Nippon Printing and Publishing Co., Ltd., Osaka, Japan, 1964.
24. Poincaré, H.: "Oeuvres," vol. 1, Gauthier-Villars, Paris, 1928.
25. Pol, B. van der: Forced Oscillations in a Circuit with Nonlinear Resistance, *Phil. Mag.,* **7-3:** 65–80 (1927).
26. Pol, B. van der: Nonlinear Theory of Electric Oscillations, *Proc. IRE,* **22:** 1051–1086 (1934).
27. Pontryagin, L. S.: "Ordinary Differential Equations," Fizmatgiz, Moscow, 1961 (in Russian); English translation, Pergamon Press, London, 1962.
28. Riasin, P.: Einstellungs- und Schwebungsprozesse bei der Mitnahme, *J. Tech. Phys.* (*USSR*), **2:** 195–214 (1935).
29. Stoker, J. J.: "Nonlinear Vibrations," Interscience Publishers, Inc., New York, 1950.
30. Whittaker, E. T., and G. N. Watson: "A Course of Modern Analysis," Cambridge University Press, London, 1935.
31. Yorinaga, M.: Bifurcation of a Periodic Solution of van der Pol's Equation with the Harmonic Forcing Term, *J. Sci. Hiroshima Univ. Ser. A-I.* **26:** 117–126 (1962).

INDEX